R. & M. No. 2987
(16,617)
A.R.C. Technical Report

MINISTRY OF SUPPLY

AERONAUTICAL RESEARCH COUNCIL
REPORTS AND MEMORANDA

The Component Pressure Losses in Combustion Chambers

By
H. A. KNIGHT and R. B. WALKER

LONDON: HER MAJESTY'S STATIONERY OFFICE
1957
TEN SHILLINGS NET

The Component Pressure Losses in Combustion Chambers

By

H. A. Knight and R. B. Walker

Communicated by the Principal Director of Scientific Research (Air), Ministry of Supply

Reports and Memoranda No. 2987*

November, 1953

Summary.—This Report summarises the available knowledge of the component losses in a combustion chamber. The information given in this Report should enable the pressure drops through swirlers, primary baffles, cooling systems, etc., to be calculated. Most of the data were abstracted and collected from the various reports listed in the bibliography. In certain cases (*e.g.*, mixing losses) the information is incomplete and in these circumstances the limited experimental results available are supplemented by hypotheses which require proof. A specimen calculation of the pressure drop and airflow distribution of a typical chamber is given in Appendix II. The calculated and measured values of pressure drop (cold) agreed within 4 per cent.

1. *Introduction.*—Effective combustion chamber design and development requires a knowledge of the airflow distribution throughout the chamber. Since the air flows through the chamber in two or three principal paths, arranged in parallel, the loss of total pressure in each path must be the same. Thus the division of air between the various paths will be determined by their relative resistances. This resistance to flow in each path is the summation of the individual component losses. For example, the primary circuit resistance comprises the swirler loss, diffusion loss, combustion loss, etc. Hence to obtain the air distribution in a given chamber the component losses must be calculable from design dimensions, and a method of combining the circuit resistances available. Such a method was developed by Probert and Kielland[1] and subsequently simplified[2] by dispensing with the ' step-by-step ' system of calculation. However, no comprehensive report on component losses has yet appeared although a note for discussion was published[3]. The present Report supplies the hitherto missing data much of which was obtained from unpublished work at the National Gas Turbine Establishment. In cases where the information is incomplete the available data are supplemented by hypotheses which require proof.

In the Report each component is considered in detail and the method of obtaining the overall loss and air distribution added for completeness. Appendix II gives a specimen calculation for a conventional chamber.

2. *Swirlers.*—Flow conditions at outlet from a swirler vary along the blade span to satisfy radial equilibrium as shown in Appendix III. Thus, free vortex blading gives a constant axial velocity component while the whirl velocity varies inversely as the radius. Other forms of blading each have their own particular characteristics. Although true mean values of the

* N.G.T.E. Report R.143, received 5th March, 1954.

velocity components should be used for pressure loss calculations, negligible error is involved and the tedium of obtaining these values obviated, by using values occurring at the weighted mean radius (r_m).

$$r_m = \frac{1}{\sqrt{2}} (R^2 + r_0^2)^{1/2} \quad \ldots \quad (1)$$

where the symbols have the significance given in Appendix I.

It is possible to study theoretically the efficiency of swirlers in turning the air through a given angle by considering the two-dimensional flow of a perfect fluid through a lattice of plates. This problem has been studied[4] and the results applied[5] to connect the angle of deviation α with the pitch/chord ratio σ for various angles of stagger β. In Fig. 1 angle of deviation is plotted against pitch/chord ratio. The curves show that for quite practical pitch/chord ratios, *i.e.*, $0 \cdot 5 < \sigma < 1 \cdot 0$ the deviation angle is almost identical with the stagger. Experimental results agree with this finding and it is now usual to employ pitch/chord ratios of about $0 \cdot 7$ for all swirlers required to give a tight swirl (*i.e.*, high values of α and β). Thus for theoretical calculations on swirler pressure losses it is both convenient and justifiable to assume that the air is deviated through the entire stagger angle β.

2.1. *Pressure Drop Due to a Swirler.*—By considering in some detail the flow through the swirler and the resultant motion of the air, an expression for the pressure drop can be derived.

Consideration is now given to the outlet flow from the swirler at the mean radius as defined by equation (1).

2.1.1. *Whirl velocity component dissipated and constant static pressure.*—Dissipation of the whirl velocity head is the most obvious assumption regarding swirler pressure drops. But an assumption must then be made about the static pressure relationship at the swirler outlet (1) and at a plane (2) situated downstream in the flame tube. A likely assumption is that the mean static pressure difference is negligible.

A mere statement of the total pressure loss is obtained by applying Bernoulli's equation, thus

$$P_1 = P_2 + \text{loss} \quad \ldots \quad (2)$$

with the further assumption of constant static pressure this reduces to

$$\text{loss} = P_1 - P_2 = \tfrac{1}{2}\rho(V_1^2 - V_2^2) \quad \ldots \quad (3)$$

and since

$$V_1 = V_a \sec \alpha$$

$$V_2 = V_a \frac{A_s}{A_F} \text{ (whirl component lost)}$$

$$\text{loss} = \tfrac{1}{2}\rho V_a^2 \left\{\sec^2 \alpha - \left(\frac{A_s}{A_F}\right)^2\right\}. \quad \ldots \quad (4)$$

Therefore

$$\Phi_F = \left\{\left(\frac{A_F}{A_s}\right)^2 \sec^2 \alpha - 1\right\}. \quad \ldots \quad (5)$$

2.1.2. *Whirl velocity component dissipated and axial momentum conserved.*—A more logical assumption than constant static pressure is conservation of axial momentum. Even this must have certain limitations since the axial momentum is unevenly distributed across the flame tube diameter and is negative along the axis due to flow reversal.

The momentum equation is

$$p_1A_s - p_2A_F + \left(\frac{p_1 + p_2}{2}\right)\left(A_F - A_s\right) = \rho A_s V_a^2 \left\{\frac{A_s}{A_F} - 1\right\} \quad \quad (6)$$

Thus
$$p_1 - p_2 = 2\left(\frac{A_s}{A_F}\right)\left(\frac{A_s - A_F}{A_s + A_F}\right)\rho V_a^2$$

and
$$\Phi_F = \left(\frac{A_F}{A_s}\right)^2 \sec^2 \alpha - 1 + 4\left(\frac{A_F}{A_s}\right)\left(\frac{A_s - A_F}{A_s + A_F}\right). \quad \quad (7)$$

2.1.3. *Consideration of most reliable assumption.*—Of these two views the former has proved to be the more reliable. Although there is the possibility of some slight pressure recovery by virtue of the area change it is undoubtedly local and is dissipated by the friction in the ensuing recirculation and general combustion turbulence. The comparison is good between measured losses given in Ref. 5 and by calculation using equation (12) which is equation (5) plus the blade loss. For typical values of A_F, A_s and α the difference in loss factor Φ_F by using equations (5) and (7) rarely exceeds 5 per cent, the former giving better agreement with experimental results. Conservation of axial and angular momentum considerably increases the difference between calculated and experimental results.

2.1.4. *Blade losses.*—In the foregoing analysis the losses are assumed to originate from the resultant flow conditions of the air after leaving the swirler and no mention was made of the losses in the swirler itself. These are due to profile and secondary losses in the blades. The former are losses attributable to skin friction and separation, the latter due to three-dimensional effects. These losses are approximately of the same magnitude and in the case of swirlers where the incidence is zero, the principal factors affecting the overall blade loss are outlet angle, pitch/chord ratio and blade passage area. However, since the blade loss represents a very small proportion of the total swirler loss, an average figure of 15 per cent of the swirler outlet velocity head is taken[6] for the blade loss for values of α in the range 65 deg $< \alpha <$ 85 deg. This figure was experimentally determined (*see* Ref. 6) and is independent of blade form.

For smaller values of α and for increased accuracy where such variables as blade height and thickness are taken into account, the following method abstracted from Ref. 7 is used.

This method is used for determining the losses in turbine nozzle guide vanes and there are obvious limitations when it is applied to swirlers. Errors are most likely to be associated with the secondary loss coefficient. Hub ratios (d/D) for turbines are of the order 0·8 whereas for swirlers they are about 0·2. Reducing the hub ratio undoubtedly increases the secondary loss for turbines and will presumably affect swirlers similarly, although to a greater degree. However, the deflection angles and flow accelerations are higher in swirlers and the latter at least will tend to reduce the loss. These various effects are allowed for (*see* section (*b*) below), but the overall impression is that the method of Ref. 8 when applied to swirlers tends to underestimate the secondary loss. Unfortunately there are not sufficient swirler tests for an independent estimate of the secondary loss to be made.

Conditions are considered at the reference radius r_m.

Details required (*see* Appendix I and Fig. 2).

(i) Blade chord, c at reference radius

(ii) Blade pitch, s at reference radius

Blade thickness $\sim t$ at reference radius

Free swirler area $\sim A_s = \pi(R^2 - r_0^2)$

(*a*) *Profile loss coefficient.*—From Fig. 3 knowing α and the pitch/chord ratio σ the profile loss coefficient Y_p is obtained.

(*b*) *Secondary loss coefficient.*—For zero incidence and assuming $\alpha = \beta$

$$\tan \alpha_n = \tfrac{1}{2} \tan \alpha \qquad (8)$$

also

$$C_L/(s/c) = 2 \tan \alpha \cos \alpha_n . \qquad (9)$$

The secondary loss for zero incidence

$$Y_s = K[C_L/(s/c)]^2[\cos^2 \alpha/\cos^3 \alpha_n] . \qquad (10)$$

The factor K is a function of $\dfrac{(A_t/A_s)^2}{\left[1 + \dfrac{d}{D}\right]}$ and is plotted in Fig. 4.

$$A_s \doteq \pi(R^2 - r_0^2)$$

$$A_t = A_n \cos \alpha \ (A_n = \text{swirler outlet area}).$$

(*c*) *Total loss coefficient* (Y_t).—

$$Y_t = Y_p + Y_s . \qquad (11)$$

If the t/s (thickness/pitch) ratio differs from $0 \cdot 02$ then the total loss coefficient should be corrected by the multiplication factor given in Fig. 5.

2.1.5. *Effect of Reynolds number on blade losses.*—The Reynolds number for a swirler is defined in the usual manner using the blade chord as the scalar length and the outlet absolute velocity, density and viscosity at the mean radius r_m. For all forms of aerodynamic machine the loss increases with decrease of Reynolds number especially in the range $R_e < 10^5$. The effect of Reynolds number on profile loss may be determined approximately from Fig. 6 which has relative loss coefficient (defined as $Y_p/(Y_p$ at $R_e = 2 \times 10^5)$ plotted against R_e and is for all forms of blading. The secondary losses are assumed to be independent of Reynolds number[8].

2.1.6. *Overall loss coefficient for a swirler.*—From equation (7) and section 2.1.4 the total loss coefficient for the swirler in terms of the flame tube area A_F is given by

$$\Phi_F = 1 \cdot 15 \left(\frac{A_F}{A_s}\right)^2 \sec^2 \alpha - 1 \qquad (12)$$

or, a little more accurately,

$$\Phi_F = \left(\frac{A_F}{A_s}\right)^2 \sec^2 \alpha \{1 + Y_t\} - 1 . \qquad (13)$$

2.1.7. *Overall loss coefficient for various types of swirler.*—Equations (12) and (13) are quite general equations for conventional swirlers and it only remains for one or two general observations to be made when these formulae are applied to the various types of swirler.

2.1.8. *Constant blade angle—curved blades.*—This type of swirler is frequently used where ' tight ' swirls are required and where the velocities are relatively high. The blades are curved so that the upstream edges are parallel to the flow, *i.e.*, zero incidence. Either equations (12) or (13) may be used to determine the loss factor (Φ_F).

2.1.9. *Constant blade angle—straight blades.*—This type of swirler is very easily manufactured and is representative of the swirlers used in large industrial-type chambers, where the overall velocities are low. Since the incidence of the blades is extremely high, the loss factor is also very high, although the flat blades are extremely effective in deviating the air through the required angle. Scanty evidence[5] suggests that the blade loss is approximately doubled compared with curved blades for the same value of α where 65 deg $< \alpha <$ 85 deg.

Hence loss coefficient for swirler with flat plates is given by

$$\Phi_F = 1{\cdot}3\left(\frac{A_F}{A_s}\right)^2 \sec^2\alpha - 1 . \qquad .. \quad .. \quad .. \quad .. \quad .. \qquad (14)$$

Obviously, the more accurate calculation of Y_t is impossible in this instance since the blades are permanently stalled due to the very high incidence.

2.1.10. *Varying Blade Angle—Curved Blades.*—In view of the manufacturing difficulties and the small increase in performance over the constant blade angle type, this type of swirler is now rarely used. The blades are usually of free vortex form giving maximum whirl velocity and hence low pressure at the centre. To apply the loss coefficient formula it is necessary to ascribe a value to sec α. As mentioned in section 2 negligible error is involved by applying values occurring at the mean radius r_m. As shown in Appendix III if the blades are of free vortex form V_a is constant and

$$\sec^2\alpha = 1 + \frac{2r_0^{\,2}}{R^2 + r_0^{\,2}}\tan^2\alpha_0$$

and

$$\Phi_F = \left[\left(\frac{A_F}{A_s}\right)^2\left(1 + \frac{2r_0^{\,2}}{R^2 + r_0^{\,2}}\tan^2\alpha_0\right)\left(1 + Y_t\right)\right] - 1 . \quad .. \quad .. \qquad (15)$$

For forced vortex blades (rarely used)

$$\sec^2\alpha = 1 + \frac{R^2 + r_0^{\,2}}{2(r_0^{\,2}\operatorname{cosec}^2\alpha_0 - R^2)}$$

and

$$\Phi_F = \left[\left(\frac{A_F}{A_s}\right)^2\left(1 + \frac{R^2 + r_0^{\,2}}{2(r_0^{\,2}\operatorname{cosec}^2\alpha_0 - R^2)}\right)\left(1 + Y_t\right)\right] - 1 . \quad .. \qquad (16)$$

2.1.11. *Ported swirler* (Fig. 7).—The development of a combustion chamber having low wall temperatures resulted in a stabilising baffle embodying this type of swirler. Assuming that the whirl and radial components of velocity are irrecoverable;

from the velocity triangle of Fig. 7

$$\text{loss} = \tfrac{1}{2}\rho(V_w^{\,2} + V_a^{\,2}\cot^2\theta) .$$

$$V_w = V_1\cos\alpha$$

$$V_a = V_a'\sin\theta = V_1\sin\alpha\sin\theta .$$

Therefore

$$\text{loss} = \tfrac{1}{2}\rho V_1^{\,2}(\cos^2\alpha + \sin^2\alpha\cos^2\theta)$$

but

$$V_1 A_s\cos\alpha = V_2 A_F$$

therefore

$$\Phi_F = \left(\frac{A_F}{A_s}\right)^2 (1 + \tan^2\alpha\cos^2\theta) \ldots \quad .. \quad .. \quad .. \quad .. \qquad (17)$$

From equation (17), as the semi-angle of the cone and the air angle through the ports relative to the tangent at the ports increase, the loss decreases. This is to be expected. There are no known experimental results from which an allowance for blade loss, *i.e.*, air friction at the ports, can be made.

2.1.12. *Tangential port swirler.*—This type of swirler was last used on the early types of chamber for the W2B, W2/500 and W2/700 engines, and may not be used in the same form again. For the purpose of determining the loss it is reasonable to assume that the velocity head through the ports is lost,

i.e., $$\Phi_F = \left(\frac{A_F}{A_s}\right)^2 . \qquad (18)$$

2.1.13. *Vortex-type swirler* (Fig. 8).—This type of swirler is basically a small vortex chamber followed by a throat and is a comparatively new type. Its ability to 'run full' gives it an advantage over the conventional swirler. With reference to Fig. 8, the pressure loss comprises two principal components. Firstly, that due to producing the whirl velocity at the throat and secondly, the production of the axial velocity component.

The pressure drop between the tangential entry and the throat is mainly a friction drop and, assuming the vortex decay law

$$V_w r^n = C ,$$

total pressure drop ΔP can be shown to be

$$\Delta P = \frac{\rho C^2}{2}\left\{\left(\frac{1}{r_2}\right)^{2n} - \left(\frac{1}{r_1}\right)^{2n}\right\}\left\{\frac{1}{n} - 1\right\} \qquad (19)$$

by integrating the equation for static pressure drop in vortex flow:

$$\frac{dp}{dr} = \rho \frac{V_w^2}{r}$$

between r_1 and r_2 and since the swirl energy at the throat is irrecoverable

$$\Delta P = \frac{\rho C^2}{2}\left\{\left(\frac{1}{r_2}\right)^{2n} - \left(\frac{1}{r_1}\right)^{2n}\right\}\left\{\frac{1}{n} - 1\right\} + \tfrac{1}{2}\rho V_{w2}^2$$

and also the axial outlet velocity must be produced.

Hence total pressure drop

$$\Delta P = \frac{\rho C^2}{2}\left\{\left(\frac{1}{r_2}\right)^{2n} - \left(\frac{1}{r_1}\right)^{2n}\right\}\left\{\frac{1}{n} - 1\right\} + \tfrac{1}{2}\rho V_{w2}^2 + \tfrac{1}{2}\rho V_a^2\left\{1 - \left(\frac{A_t}{A_F}\right)^2\right\}$$

also by continuity

$$V_{w1}A_s = A_t V_a = A_F V_F . \qquad (20)$$

Therefore

$$\Delta P = \frac{\rho V_{w1}^2}{2}\left[\left(\frac{r_1}{r_2}\right)^{2n}\frac{1}{n} - \left(\frac{1}{n} - 1\right) + \left(\frac{A_s}{A_t}\right)^2\left\{1 - \left(\frac{A_t}{A_F}\right)^2\right\}\right], \qquad (21)$$

thus

$$\Phi_F = \left(\frac{A_F}{A_s}\right)^2\left[\left(\frac{r_1}{r_2}\right)^{2n}\frac{1}{n} - \left(\frac{1}{n} - 1\right) + \left(\frac{A_s}{A_t}\right)^2\left\{1 - \left(\frac{A_t}{A_F}\right)^2\right\}\right]. \qquad (22)$$

For a free vortex $n = 1$, but tests on a model cyclone of approximately 18-in. maximum diameter and 6-in. wide have shown $n = 0 \cdot 95$, and that n decreases further as the width is reduced. Since for a practical size of swirler the effective Reynolds number is lower and the wetted area/flow area ratio is greater, n will probably be of the order $0 \cdot 8$. No experimental results are available for confirmation of this value. The angle of swirl at the throat ω is given by

$$\omega = \tan^{-1}\frac{V_{w2}}{V_{a2}} ,$$

i.e., $$\tan \omega = \left(\frac{r_1}{r_2}\right)^n \frac{A_t}{A_s} . \qquad (23)$$

Thus a wide latitude is allowed in designing a vortex swirler for a given value of swirl angle.

2.2. *Swirler Followed by a Throat.*—The combination of a swirler followed by a throat occurs frequently in chambers containing ceramic liners. This problem was studied[9] and predicted values for the pressure loss were closely substantiated by experimental results. The problem is complicated by the fact that heat addition occurs at the reference planes downstream from the swirler exit. With reference to the notational diagram Fig. 9:

Axial velocity from swirler outlet $= \frac{A_F}{A_s}\frac{\rho'}{\rho} V_F$, ... (24)

Whirl velocity from swirler outlet $= \frac{A_F}{A_s}\frac{\rho'}{\rho} V_F \tan\alpha$ . .. . (25)

The kinetic energy changes between the plane of the swirler outlet and the ceramic liner throat are based on the assumptions that the axial velocity component increases in the ratio of the areas and the whirl velocity in the square root of this ratio, making it a type of free vortex. This latter assumption implies that the moment of momentum is constant on a stream surface and is described in Ref. 5.

Axial velocity at throat $= \frac{A_F}{A_t} V_F \frac{\rho'}{\rho''}$ .. .. (26)

Whirl velocity at throat $= \frac{A_F}{A_s}\sqrt{\left(\frac{A_s}{A_t}\right)}\frac{\rho'}{\rho''} V_F \tan\alpha$ . .. . (27)

Thus assuming no pressure recovery and the static pressure difference to be negligible between the throat and the flame tube downstream

$$\text{loss} = \tfrac{1}{2}\rho'' V_t^2 - \tfrac{1}{2}\rho' V_F^2$$

$$= \tfrac{1}{2}\rho''\left\{\left(\frac{\rho'}{\rho''}\right)^2\left(\frac{A_F}{A_s}\right)^2\frac{A_s}{A_t}\cdot V_F^2\tan^2\alpha + \left(\frac{A_F}{A_t}\right)^2 V_F^2\left(\frac{\rho'}{\rho''}\right)^2\right\} - \tfrac{1}{2}\rho' V_F^2$$

$$= \tfrac{1}{2}\rho' V_F^2\left[\frac{\rho'}{\rho''}\left\{\left(\frac{A_F^2}{A_s A_t}\right)\tan^2\alpha + \left(\frac{A_F}{A_t}\right)^2\right\} - 1\right]. \quad \text{.. .. .. .. (28)}$$

The blade loss in the swirler is

$$Y_t\left\{\tfrac{1}{2}\rho\left(\frac{A_F}{A_s}\frac{\rho'}{\rho} V_F \sec\alpha\right)^2\right\}. \quad \text{.. .. .. (29)}$$

Overall loss factor obtained by combining equations (28) and (29) and simplifying

$$\Phi_F = \left[\left(\frac{\rho'}{\rho''}\right)\left(\frac{A_F}{A_t}\right)^2\left\{\frac{A_t}{A_s}\tan^2\alpha + 1\right\} + Y_t\left(\frac{\rho'}{\rho}\right)\left(\frac{A_F}{A_s}\right)^2\sec^2\alpha\right] - 1 \ldots \quad \text{.. .. (30)}$$

In equation (30) Y_t is determined by the methods given in sections 2.1.4, 2.1.5 and 2.1.9.

In the design or project stage, it is difficult to ascribe values to ρ'' i.e., the density at the throat. However, the density relationship throughout the primary zone may be written:

$$\left(\frac{1}{\rho''} - \frac{1}{\rho}\right) = G\left(\frac{1}{\rho'} - \frac{1}{\rho}\right) \quad \text{.. .. .. (31)}$$

which is based on a temperature relationship assuming constant static pressure. G is a factor ($0 < G < 1$) depending upon the amount of heat release between the exit of the swirler and the throat. The value of $\rho/\rho' = x$ say, can usually be fixed with a reasonable accuracy, and equation (31) reduces to

$$\frac{\rho''}{\rho} = \frac{1}{G(x-1)+1}. \quad \text{.. .. .. (32)}$$

By substituting probable values for G, ρ'' is obtained. In practice it is doubtful if G will exceed $0 \cdot 5$ and generally $0 \cdot 25 < G < 0 \cdot 5$. In a previous analysis[9] taking values of G of $0 \cdot 25$ and $0 \cdot 5$ varied the primary loss factor some 30 per cent and the overall loss factor some 7 per cent. Thus the value ascribed to G is not really critical in determining the overall loss of the chamber.

3. *Primary Stabiliser Losses.*—The fundamental principle of flame stabilisation is to reduce the local velocity and effect a flow reversal by which fresh mixture is added to the piloting region to propagate combustion. This is achieved by two distinct forms of piloting system, *viz.*, gutter and plain baffle-type stabilisers. The former type are used where high velocity conditions exist, *i.e.*, ram jets, reheat, etc., and although considerable work is being carried out on gutters few published notes are available. The plain baffle-type stabilisers incorporating a swirler are used in the majority of aero-engine and industrial-type chambers.

3.1. *Plain Baffles.*—These plain baffles are of varying form although they do preserve some symmetry in design. To obtain the complete baffle loss the pressure loss of the various free area shapes (holes, scoops, etc.), which constitute the baffle must be determined. When air flows through these various holes the issuing free jets are conoidal in shape and hence give rise to a discharge coefficient. If $C_{d\,0}$ and A_0 are the overall discharge coefficient and total free area of the baffle respectively and the various components have free areas A_1, A_2, A_3 . . . . . and discharge coefficients $C_{d\,1}$, $C_{d\,2}$, $C_{d\,3}$ . . . . . .

then
$$C_{d\,0} = \frac{A_1 C_{d\,1} + A_2 C_{d\,2} + A_3 C_{d\,3} \ldots .}{A_1 + A_2 + A_3 \ldots .}$$
$$= \frac{\Sigma A C_d}{\Sigma A} . \qquad (33)$$

Thus any shape or size of baffle can be reduced to the simple case of an equivalent hole in a flat plate. The necessary experimental values of discharge coefficient are taken from experimental results obtained at N.G.T.E[10]. Briefly, the various baffles were mounted in a test section and the loss of total pressure measured for a range of velocities. Theoretically[11], the pressure loss is calculable providing the free area of the baffle, the cross-sectional area to which the flow expands (in terms of area, since this is actually a diffusion process) and the discharge coefficient are known. The former values are obtained by actual measurement but the discharge coefficient can only be determined experimentally.

3.2. *Variables Affecting the Pressure Loss of Plain Baffles.*—3.2.1. *Effect of velocity.*—The theoretical curves[11] show that the non-dimensional loss factor increases with Mach number which for constant static temperature is proportional to the velocity. Pressure loss tests on various baffle shapes have shown that the loss does in fact increase with Mach number but at a reduced rate of increase to that predicted. It was thought that an increase in the discharge coefficient with Mach number might account for the discrepancy and this has now been substantiated by independent experiments[12]. Variation of C_d with vena-contracta Mach number is shown in Fig. 10. For most combustion chambers the change of C_d is small, but since the loss is inversely proportional to C_d^2 its effect will be significant.

3.2.2. *Effect of area ratio.*—For a given shape of hole the discharge coefficient increases initially almost as the square of the area ratio as shown in Fig. 11 in which the relative coefficient is plotted against area ratio. This curve is based on values obtained from Ref. 13 and by experiment and is for sharp-edged circular orifices. The equivalent curve for other shapes of orifice will be slightly different.

3.2.3. *Effect of hole size.*—The effect of using baffles containing a similar total area of holes of different size has not resulted in any definite conclusions being reached. A large number of small holes would be expected to give a higher loss on account of the larger wetted area available for friction. However, experimental results show the converse to be true, *i.e.*, the baffle having a small number of large holes has a 2 per cent higher pressure loss. It should be appreciated that the experimental error is of this order and also variation in the diameter of the holes has to be extremely small to account for this difference.

3.2.4. *Effect of hole shape.*—The shape of the hole for a given free area does affect the pressure loss by variation in the discharge coefficient. Circular holes have the lowest discharge coefficient for a given free area. Square orifices have slightly higher values of C_d and rectangular and elliptical orifices with high values of major/minor axis ratio higher values still. Typical minimum values, *i.e.*, corresponding to infinite area ratio, are given in Table 1 below.

TABLE 1

Type	Circular	Square	Rectangular	Elliptical	Elliptical
Axis ratio	—	1	3 : 1	2 : 1	4 : 1
C_d	0·60	0·62	0·63	0·62	0·63
Hydraulic mean depth ..	$0{\cdot}282\sqrt{A}$	$0{\cdot}25\sqrt{A}$	$0{\cdot}214\sqrt{A}$	$0{\cdot}26\sqrt{A}$	$0{\cdot}204\sqrt{A}$

The vena-contracta is formed by the inward radial flows on the upstream face of the baffle acting on the jet periphery. For a hole in the centre of the baffle these contracting forces are strongest when acting normal to the jet surface. For a circular hole the forces act normal to the surface over the entire periphery and produce the greatest contraction. Thus contraction coefficient (C_c) increases as the hole shapes become 'less circular', *i.e.*, elliptical (2 : 1), square, rectangular, etc.

C_v, velocity coefficient, represents the ratio of actual to theoretical velocity through the hole and is due to viscosity and boundary friction. Hence increasing the periphery of a hole for a given cross-sectional area results in a decrease of C_v. For holes in thin plates C_v tends to unity and as periphery variations (as shown in Table 1 where hydraulic mean depth $= \frac{\text{cross-sectional area}}{\text{periphery}}$) are small, changes in C_v are negligible. Since discharge coefficient $= C_d = C_c C_v$ changes in C_c will be the predominating factor. Thus for maximum discharge through a given area the hole shape should be rectangular with, for example, an axis ratio of 4 : 1. However, practical disadvantages such as corner stress concentrations and manufacturing difficulties may outweigh the advantage of the small increase in (C_d).

For an annulus around a hemispherical baffle mean values of 0·9 for the discharge coefficient were obtained.

'Thumbnail' scoops have a discharge coefficient closely approaching unity.

3.2.5. *Effect of hole arrangement.*—No general conclusions may be drawn from the disposition of holes in a baffle. Various arrangements of holes, for a constant area ratio, lead to negligible changes in the overall loss factor.

3.2.6. *Effect of hole inclination.*—To determine the effect of inclination of the plane of the hole to the air stream a series of cones were tested in which the cone angle was varied but the area ratio and hole arrangement remained the same. When the holes were placed normal to the air-stream minimum loss was obtained. As the angle between the axes of the holes and the air stream θ increased the loss increased approximately as $\cos^2 \theta$ as shown in Fig. 12. This is to be expected since the projected area of the holes on a plane normal to the airflow is directly proportional to $\cos \theta$ and loss is proportional to the square of the area ratio. Fig. 13 shows relative loss defined as $\frac{\text{loss factor at inclination } \theta}{\text{loss factor at } \theta = 0 \text{ (\textit{i.e.}, minimum loss)}}$ plotted against θ. Placing the cone apex upstream or downstream had no measurable effect on the loss.

3.2.7. *Effect of turbulence.*—Ref. 14 gives details of experiments carried out on a series of flat plates which illustrate the effect of turbulence on drag. Fig. 14 shows the variation of pressure drop coefficient (static-pressure difference/free-stream velocity head) with percentage turbulence. The percentage turbulence is defined as

$$\frac{\text{root mean square of speed fluctuation}}{\text{average speed}} \times 100$$

The turbulence level was varied by placing large-wire-diameter, large-mesh gauzes upstream of the test section. Considering practical applications, the change of percentage turbulence is usually small in a given test set-up, but this feature of drag increase with percentage turbulence is important when comparing pressure loss measurements made on an identical component on two dissimilar rigs. However, reference to Fig. 14 shows that percentage turbulence changes will only account for small differences in pressure loss.

3.3. *Gutter Stabilisers.*—The loss due to gutters is mainly an expansion loss arising from the fuel injector situated in the high-velocity throat and also the diffusion loss up to the chamber cross-section from the downstream end of the gutter. For incompressible flow the loss is $(\lambda - 1)^2$ and includes a discharge coefficient for the gutter. For included gutter angles up to 15 deg the value of C_d is about unity. For higher angles the C_d decreases fairly rapidly, probably following a cosine law, but this is merely a hypothesis which, although qualitatively correct, should be confirmed experimentally before being used indiscriminately. If the throat velocity is greater than 200 ft/sec the curves of Ref. 11 should be used to allow for compressibility in determining the pressure loss.

For hot running the fundamental pressure loss due to heat addition (*see* section 6) is added to the cold loss. The result obtained may be high compared with the experimental value. This is due to the aerodynamic flow pattern around the gutter being significantly altered by combustion. The principal effects of combustion are to reduce the strength of the reverse flow (and hence the pressure loss) and to increase the length and breadth of the wake. A further contribution to the loss factor is the dissipation of the upstream component of the fuel momentum when injected in the throat. If the inlet air and fuel temperatures are substantially the same, increase in fuel flow results in an increase in pressure loss (of the order 3 to 5 per cent), but if the air temperature is high compared with the fuel the pressure loss tends to decrease. This latter phenomenon is due to the reduction in air temperature due to fuel vaporisation. The presence of the fuel increases the effective blockage at the throat, and since the throat velocity and permanent blockage are both high, exerts a measurable effect on the loss. If the throat section is long friction effects must be taken into account by the modified ' Fanning equation '

$$\frac{d(\Delta P)}{dl} = 4\,\frac{f}{D} \cdot \tfrac{1}{2}\rho V^2 \qquad \text{(34)}$$

for rectangular or annular cross-sectional areas the equivalent diameter (d_e) is used. f will vary between 0·002 and 0·008 depending on the Reynolds number as shown in Fig. 15.

The effect on pressure loss of using skirted gutters (*see* Figs. 16a and 16b) as opposed to the conventional type is negligible, although an improvement in flame stability may result. The use of ' finger ' type flame spreaders attached to the downstream end of the gutter gives rise to a small increase in the loss which is accounted for approximately by the loss due to flow through the projected free area of the fingers in the plane of the gutter base as shown in Fig. 16c. This loss will probably be a little higher than the more gradual loss occurring along the fingers, but does give a basis for analytical determination. Diffusion losses can be treated by the method given in section 7.1.

From the preceding paragraph it is obvious that the pressure loss picture is far from complete, but correlation of the results of many experiments now in progress will improve the position.

4. *Cooling Losses.*—The main types of cooling device in use at the present time are the louvre, porous wall and boundary-layer systems. For a detailed analysis and description of these systems Ref. 15 should be consulted. From the point of view of pressure loss no new problems are involved, each system merely utilising the available pressure difference between the primary and secondary flow paths.

4.1. *Porous Wall.*—This method of cooling is among the more efficient and is amenable to analytical treatment. The pressure drop for laminar flow through a porous material is given by D'Arcy's equation

$$\frac{QL}{p_1^2 - p_2^2} = \frac{Z}{144} \frac{\rho_2}{2p_2\mu} \qquad (35)$$

where p_1 and p_2 are the air pressures in lb/ft^2 on either side of the porous wall and Z is the coefficient of permeability and has dimensions of an area, usually square inches. For the small pressure differences available in combustion chambers

$$p_1^2 - p_2^2 \simeq 2p_2 \, \Delta p \text{ where } \Delta p = \text{pressure drop}$$

thus

$$\frac{QL}{\Delta p} = \frac{Z}{144} \frac{\rho}{\mu} . \qquad (36)$$

However, Z must be determined experimentally in the first instance, and may decrease with operating time due to deposition in the pores. Typical values of Z are 10^{-8} to 10^{-10} in^2.

4.2. *'Louvred' Surface Cooling.*—The 'louvred' wall is essentially a mode of construction (British Patent No. 642,257 held by 'Shell' Refining and Marketing Company Limited) by which the effective area for heat transfer is considerably increased. The surface to be cooled is constructed so that there are many small independent passages along which the cooling air may flow radially, finally emerging to mix with the primary stream. To estimate the pressure drop associated with the flow of air through the passages in the 'louvred wall' under turbulent flow conditions, Blazius' equation is used:

$$\Delta P = \frac{0 \cdot 316}{R_e^{0 \cdot 25}} \frac{\rho V^2}{2} \frac{L}{d_e} . \qquad (37)$$

For laminar-flow conditions:

$$\Delta P = \frac{96}{R_e} \frac{\rho V^2}{2} \frac{L}{d_e} . \qquad (38)$$

The criterion for turbulent or laminar flow is whether R_e is above or below 2,000. In addition the injection loss $= \frac{1}{2}\rho V^2$ should be added to either equation (37) or (38) to give the complete loss.

4.3. *Combination of External Airflow and Localised Air Injection Cooling.*—This method requires the cooling air to flow in an annular sheath in an upstream axial direction and then to inject it through small holes in the flame tube into the high temperature side where it forms a blanketing annular layer. The pressure drop is the sum of the friction drop given by equations (37) or (38) and the injection loss which will be due to accelerating the air up to the required injection velocity. The latter loss is given by

$$\Delta P = \tfrac{1}{2}\rho \left(\frac{V_h}{0 \cdot 61}\right)^2 \qquad (39)$$

where V_h is the velocity based on total port area and $0 \cdot 61$ is the discharge coefficient.

The overall loss for this cooling system is

$$\Delta P = \frac{0 \cdot 316}{R_e^{0 \cdot 25}} \frac{\rho V^2}{2} \frac{L}{d_e} + \frac{\rho}{2}\left(\frac{V_h}{0 \cdot 61}\right)^2 . \qquad (40)$$

5. *Mixing Losses.*—Up to this section most of the information is complete and valid for all types of combustion chamber but an incomplete knowledge of the mixing process restricts the application to low-speed chambers.

The pressure loss due to mixing is probably the most difficult loss to determine analytically without some experimental assistance, since it affects both the primary and secondary streams. The part of the mixing loss attributable to the secondary circuit is almost entirely due to expansion through the mixing holes. The loss associated with the primary circuit is made up of the flow through the effective blockage due to the radial ' spokes ' of cold air and the subsequent macro-turbulence.

5.1. *Secondary Mixing Losses.*—As stated in the previous section the secondary mixing loss is given approximately by the velocity head through the holes. This requires a knowledge of the discharge coefficient, which is subject to a wide variation depending on hole area, outer duct area and the percentage flow from the outer duct through the hole. Fig. 17 is a curve of C_d versus a factor F/B where F is the percentage flow from the outer duct and B is the ratio of hole area/outer duct area. This curve was taken from Ref. 16 and is the result of water model tests with hole sizes ranging from 0·6 to 1·9 in. diameter. It is satisfactory to determine the percentage flow through the hole on an area basis.

Darling[17] has also studied this problem using air as the flow medium and presents his values of discharge coefficient as a function of the ' Approach velocity factor ', *i.e.*, V_1/V_2 where V_1 is the mean velocity in the approach channel, and V_2 is the mean velocity through the hole. The number of experimental points taken are less than in Ref. 17 and only one size of hole was used. Darling's results have been plotted on the same abscissa as the Lucas results in Fig. 17. The curves are of similar shape although the curve for air is some 7 per cent higher. For equal conditions of flow the discharge coefficient for air would be higher due to compressibility although by a very small amount. The real difference appears to be due to the positioning of the static taps on the two separate rigs. For the water model they are situated in the annulus some $2\frac{3}{4}$-in. upstream of the injection hole axis whereas for the air tests the tap was situated on the outer annulus wall directly above the centre of the hole. The maximum value of C_d obtained in Ref. 17 is higher than anticipated for this type of discharge. The true values for air are probably a little higher than the water results although negligible error will result in applying these directly to air calculations*.

The secondary pressure loss due to mixing will then be given by

$$\Delta P = \tfrac{1}{2}\rho\left(\frac{V_h}{C_d}\right)^2, \qquad \ldots \qquad (41)$$

C_d being obtained from Fig. 17.

For holes inclined to the direction of flow the discharge coefficient obtained from Fig. 17 should be increased by the root of the relative loss factor since $C_d \propto 1/\Phi$. For example, if the mixer has a semi-angle of 15 deg then with reference to Fig. 13, $\theta = 75$ deg, and C_d obtained from Fig. 17 is multiplied by $\sqrt{(1\cdot482/1\cdot452)}$.

The preceding statements assume that the hot-stream effects are negligible. This is probably true for low-speed industrial-type chambers but evidence from experiments now in progress suggests that the hot-stream momentum substantially affects the result and reduces the value of the pressure drop as given by equation (41).

5.2. *Primary Mixing Losses.*—Losses in the hot stream from the injection plane to the ' mixed ' plane are approximately half the velocity head at the plane of injection and are thus very small. For very large or industrial-type chambers it can be regarded as negligible. This part of the work will be in a much more exact form when the results of mixing experiments now in progress are available.

* This statement is confirmed by an American Report ' Can burner hole discharge coefficient investigation ', Consolidated Vultee Aircraft Corporation No. 6149, just received.

6. *Heat Addition Losses.*—If, as is usual, the combustion occurs in a parallel duct immediately downstream of the primary baffle the 'fundamental' loss of pressure is given by

$$\Delta P = \tfrac{1}{2}\rho_1 V_1^2\left(\frac{\rho_1}{\rho_2} - 1\right) \quad \ldots \quad (42)$$

and if the static pressure difference is small

$$\Delta P = \tfrac{1}{2}\rho_1 V_1^2\left(\frac{T_2}{T_1} - 1\right). \quad \ldots \quad (42a)$$

In the case of a varying cross-sectional area in the flame tube, it is best to consider in detail the relative proportions of heat release as in section 2.2.

7. *Miscellaneous Losses.*—7.1. *Diffusion Losses.*—For various reasons the reduction of velocity in the compressor diffuser is often limited and the inlet velocity to the combustion chamber is frequently greater than 300 ft/sec, the exact value depending to a large extent on the type of compressor. Typical values for the velocity in the secondary annulus are of the order of 150 ft/sec and it is necessary to reduce the inlet air velocity to that existing in the secondary annulus as efficiently as possible. The efficiency of a diffuser may be defined by a factor e which gives the efficiency of conversion of velocity head to static pressure.

Thus

$$p_2 - p_1 = e\frac{\rho}{2g}(v_1^2 - v_2^2). \quad \ldots \quad (43)$$

Therefore

$$\text{total pressure loss } P_1 - P_2 = (1 - e)\frac{\rho}{2g}(v_1^2 - v_2^2) \quad \ldots \quad (44)$$

$$\text{loss factor } \Phi = (1 - e)\left\{1 - \left(\frac{A_1}{A_2}\right)^2\right\}. \quad \ldots \quad (45)$$

Values of e have been taken from Ref. 18 which agree with experimental results given in Ref. 19 and are plotted in Fig. 18 against total diffuser angle θ. A recent report[20] has shown that asymmetry of the inlet velocity distribution has a marked effect on diffuser efficiency especially for large diffuser angles. A low velocity region near the wall is equally undesirable.

7.2. *Losses Due to Bends.*—Although not explicitly a component of the combustion chamber, bend entries and exits for combustion chambers are relatively common and their loss is frequently included in the overall chamber loss figure. Accurate data for the losses in bends is given in Ref. 21, but in general terms it can be stated that, for a bend without diffusion and with a directional change not exceeding 90 deg, and having a mean radius not less than 1·5 times the duct diameter or passage width, the pressure loss will not exceed half the velocity head. The loss round a sharp bend can be reduced by imparting an acceleration to the air.

Cascade bends are now universally employed in gas turbine systems by virtue of their efficiency both in terms of pressure drop and their ability to turn the air through a desired angle. Ref. 22 gives the design details and procedure for constructing a bend in which the blades are spaced in an arithmetic progression from the inside radius. The pressure loss associated with such a bend is affected by size and manufacturing variations (especially internal finish) but a loss figure of 25 per cent of the velocity head through the bend is sufficiently accurate for most purposes.

7.3. *Losses Due to Corrugated Spacers.*—This form of construction is now used frequently as a mechanical spacer for skin cooling of combustion chamber walls. The discharge coefficient of this spacer was investigated[23] on a water model and found to be 0·8 when based on the drawing dimensions and 0·9 in terms of the actual measured areas. The variation in drawing and measured dimensions is due to manufacturing difficulties principally in the welding operation. For design purposes the estimated area of the section is used for which C_d equals 0·8.

7.4. *Friction Losses.*—In the majority of chambers the friction losses are usually negligible compared with the individual component losses but in a few isolated cases there are long sections where frictional affects are measurable.

The pressure drop is given by the modified ' Fanning equation '

$$\frac{d(\Delta P)}{dl} = 4\frac{f}{D}\cdot\tfrac{1}{2}\rho V^2 , \quad \ldots \quad \ldots \quad \ldots \quad \ldots \quad \ldots \quad \ldots \quad (34)$$

f being obtained from Fig. 15.

For irregular shaped ducts and annuli the hydraulic mean diameter d_e is used for D,

i.e., $$D = 4\frac{A}{S} .$$

8. *Overall Chamber Loss.*—Having considered in some detail the pressure losses caused by the various components of the chamber, it is now necessary to see how they may be linked to give a value of the loss coefficient for a particular flow path. For consecutive losses in a flow path the overall loss coefficient is merely the arithmetic sum of the individual loss factors provided they are expressed in terms of the same reference velocity head. For losses occurring in parallel circuits the method of Probert and Kielland[1] is used. A loss coefficient is applied to each flow path such that the total-head loss in the stream is equal to the loss coefficient times the velocity head at some reference area. On the further assumption that the static pressures are equal in both streams at divergence and confluence an expression for the overall loss factor is obtained. While this method proves satisfactory for the simpler types of chamber a considerable amount of calculation is required if there are more than two general flow paths. Also, because of the 'step-by-step ' method of calculation, if the loss factor of one of the components is changed a complete recalculation is necessary.

Ref. 2 is based on the same principles and assumptions as stated above but as shown in Appendix II reduces the complexity and quantity of calculation.

If ϕx = pressure loss factor of a circuit in terms of velocity head at area x

and ϕy = same loss in terms of velocity head at area y

then
$$\frac{\phi x}{\phi y} = \left(\frac{x}{y}\right)^2 \quad \ldots \quad \ldots \quad \ldots \quad \ldots \quad \ldots \quad \ldots \quad \ldots \quad (46)$$

and in the event of a density change

$$\frac{\phi x}{\phi y} = \left(\frac{x}{y}\right)^2\left(\frac{\rho_y}{\rho_x}\right) . \quad \ldots \quad \ldots \quad \ldots \quad \ldots \quad \ldots \quad \ldots \quad (47)$$

Thus by applying this relation it is possible to express all individual loss factors in terms of the velocity heads, due to each flow, at the same cross-sectional area. This reference area is purely arbitrary and can be the chamber-entry area, flame-tube area or casing area.

When air flows through the individual flow paths arranged in parallel, the loss of total pressure along each path must be the same. If all but one of the flow paths are blanked off, and we assume that air flows along this one path until the pressure loss has the same value as that when air is flowing in equilibrium through all the paths, there will be a velocity head q_1 at the reference area and a corresponding loss factor ϕ_1. Treating the other flow paths similarly, we obtain

$$\phi_1 q_1 = \phi_2 q_2 = \phi_3 q_3 = \Phi q . \quad \ldots \quad \ldots \quad \ldots \quad \ldots \quad \ldots \quad (48)$$

where q_1, q_2 . . . etc. are the velocity heads due to the individual flows in the reference area, and ϕ_1, ϕ_2 . . . etc. are the loss factors expressed in terms of the velocity head at the reference area by means of equation (47).

But $q \propto W^2$ since ρ is assumed constant at the reference area for all flows.

Therefore
$$W_1\sqrt{\phi_1} = W_2\sqrt{\phi_2} = W_3\sqrt{\phi_3}, \text{ etc.,} \qquad \qquad (49)$$

and the overall loss factor is given by

$$\Phi = \phi_1\left(\frac{W_1}{W}\right)^2 = \phi_2\left(\frac{W_2}{W}\right)^2, \text{ etc.} \qquad \qquad (50)$$

Also since the sum of the percentage flows through each circuit must equal the total flow

$$W = 100 \doteq W_1 + W_2 + W_3\,, \text{ etc.} \qquad \qquad (51)$$

Thus any required circuit flow say W_1 is given by:

$$W_1 = 100 - W_2 - W_3$$

$$= 100 - W_1\left(\frac{\phi_1}{\phi_2}\right)^{1/2} - W_1\left(\frac{\phi_1}{\phi_3}\right)^{1/2}$$

$$W_1 = \frac{100}{1 + \left(\frac{\phi_1}{\phi_2}\right)^{1/2} + \left(\frac{\phi_1}{\phi_3}\right)^{1/2}}. \qquad \qquad (52)$$

Also
$$\Phi = \frac{\phi_1}{\left[1 + \left(\frac{\phi_1}{\phi_2}\right)^{1/2} + \left(\frac{\phi_1}{\phi_3}\right)^{1/2}\right]^2},$$

assuming there is a total of three circuits.

9. *Conclusions.*—By means of the analysis of component pressure losses in this Report it should be possible to make a reasonably accurate theoretical calculation of the cold airflow distribution and overall loss factor of a combustion chamber. Certain limitations in our knowledge of compressible flow characteristics, especially mixing of gas streams, imposes a restriction on the accuracy for high velocity chambers. This contingency will be obviated by experimental work now in hand. The comparison between calculated and measured pressure drop for a typical combustion chamber as shown in Appendix II is good. The percentage difference may be fortuitous but the prospects of calculating the cold pressure drop of a chamber from the design drawing with an accuracy of $\pm$ 5 per cent seems favourable. Assuming the mixing experiments improve the 'hot' pressure loss calculations, the method can probably be further refined by comparing calculated and measured results from a variety of chambers.

REFERENCES

No.	Author	Title
1	R. P. Probert and A. Kielland ..	Experiments on combustion chamber pressure loss. Power Jets Report R.1164. December, 1945.
2	R. B. Walker	Unpublished work at N.G.T.E.
3	H. A. Knight	Unpublished work at N.G.T.E.
4	W. F. Durand	*Aerodynamic Theory.* Vol. 2, pp. 91 to 96. Reprinted, January, 1943.
5	I. Berenblut	The pressure losses in combustion chambers with swirl air directors. Shell Report ICT/20. December, 1948.
6	D. G. Ainley and G. C. R. Mathieson	An examination of the flow and pressure losses in blade rows of axial-flow turbines. R. & M. 2891. March, 1951.
7	D. G. Ainley and G. C. R. Mathieson	A method of performance estimation for axial-flow turbines. R. & M. 2974. December, 1951.
8	D. G. Ainley	*Proc. Inst. Mech. Eng.* Vol. 159 (W.E.I. No. 41). 1948.
9	R. P. Probert and H. A. Knight ..	Unpublished work at N.G.T.E.
10	H. A. Knight	Unpublished work at N.G.T.E.
11	H. A. Knight	Theoretical investigations into baffle pressure losses. N.G.T.E. Memo. M. 52. A.R.C. 12,708. June, 1949.
12	E. E. Callaghan and D. T. Bowden ..	Investigation of flow coefficient of circular, square and elliptical orifices at high pressure ratios. N.A.C.A. Tech. Note 1947. September, 1949.
13	—	B.S. Code 1042. Flow measurement. 1943.
14	G. B. Schubauer and H. L. Dryden ..	The effect of turbulence on the drag of flat plates. N.A.C.A. Report 546. 1935.
15	F. J. Bayley	Air cooling methods for gas turbine combustion systems. C.P. 133. August, 1951.
16	D. J. Miller	The coefficient of discharge of a circular hole in the wall of a duct. Lucas Report B.41, 349. January, 1951.
17	R. F. Darling	Tests on the flow of dilution air through a hole in a flame tube. Pametrada Report No. 52. November, 1949.
18	N. A. Hall	*Thermodynamics of Fluid Flow.* Wiley and Co. 1951.
19	A. H. Gibson	*Hydraulics and its Applications.* 4th Edition. Constable & Co., Ltd. 1946.
20	I. H. Johnson	The effects of inlet conditions on the flow in annular diffusers. C.P. 178. January, 1953.
21	S. Gray	A survey of existing information on the flow in bent channels and the losses involved. Power Jets Report R.1104. June, 1945.
22	N. A. Dimmock	The development of a simply constructed cascade corner for circular cross-section ducts. N.G.T.E. Memo. M.78. A.R.C. 13,369. February, 1950.
23	D. J. Miller	The coefficient of discharge of a gap containing a corrugated spacer. Lucas Report B.41,689. March, 1952

APPENDIX I

List of Symbols

A	Cross-sectional area (ft^2)
B	Ratio $\dfrac{\text{hole area}}{\text{outer duct area}}$ (*see* Fig. 17) (dimensionless)
C	Constant for vortex decay law
c	Blade chord
C_d	Discharge coefficient (dimensionless)
C_L	Lift coefficient (*see* equations 9 and 10) (dimensionless)
D	Outer diameter (ft)
d	Inner diameter (ft)
d_e	Equivalent diameter $= 4 \times \dfrac{\text{cross-sectional area}}{\text{perimeter}}$ (ft)
e	Diffuser efficiency (dimensionless)
F	Percentage flow from outer duct (*see* Fig. 17) (dimensionless)
f	Friction factor (*see* equation 34) (dimensionless)
G	Heat release factor (*see* equation 31) (dimensionless)
H	Total energy per unit mass (ft^2 sec^{-2})
K	Secondary loss factor (*see* equation 10) (dimensionless)
L, l	Length (ft)
M	Mach number (dimensionless)
M_v	Mach number at vena-contracta (dimensionless)
m	Area ratio $= d^2/D^2$ (dimensionless)
n	Index in vortex decay law (dimensionless)
P	Total pressure (lb/ft^2)
p	Static pressure (lb/ft^2)
ΔP	Total pressure loss (lb/ft^2)
Δp	Static pressure loss (lb/ft^2)
Q	Mass flow per unit cooled surface area (slugs sec^{-1} ft^{-2})
R, r	Radii (ft)
R_e	Reynolds number (dimensionless)
S	Perimeter (ft)
s	Pitch (ft)
t	Blade thickness (ft)

V	Absolute velocity (ft/sec)
V_a	Axial velocity (ft/sec)
V_h	Velocity through hole (ft/sec)
V_w	Whirl velocity (ft/sec)
W	Weight flow (lb/sec)
x	Area (ft^2)
Y_p	Profile-loss coefficient (dimensionless)
Y_s	Secondary-loss coefficient (dimensionless)
Y_t	Total-loss coefficient (dimensionless)
y	Area (ft^2)
Z	Coefficient of permeability (*see* equation (36)) (in^2)
α	Outlet air angle (dimensionless)
β	Blade outlet angle (dimensionless)
γ	Ratio of specific heats (dimensionless)
θ	Baffle semi-cone angle (dimensionless)
λ	Effective area ratio (dimensionless)
μ	Viscosity (slugs ft^{-1} sec^{-1})
ρ	Density (slugs ft^{-3})
ρ'	Flame tube density (*see* Fig. 9) (slugs ft^{-3})
ρ''	Throat density (*see* Fig. 9) (slugs ft^{-3})
σ	Pitch/chord ratio $= s/c$ (dimensionless)
Φ, ϕ	Loss coefficient $= (P_1 - P_2)/\frac{1}{2}\rho_1 V_1^2$ (dimensionless)
ω	Swirl angle for vortex swirler (*see* section 2.1.13) (dimensionless)

Suffices

$_0$	Known condition, usually inner radius
$_1$	Entry or initial condition
$_2$	Outlet or final condition
$_F$	Pertaining to flame tube
$_m$	Pertaining to mean radius
$_s$	Pertaining to swirler or secondary
$_t$	Throat condition

APPENDIX II

Airflow Distribution and Overall Loss Factor for a Conventional Chamber
(Rolls Royce R.M.60 Model)

As can be seen from Fig. 19 the airflow is divided into eight separate flow circuits. Each individual loss factor will be expressed in terms of the velocity head pertaining to the overall chamber cross-sectional area.

To determine the ' hot ' distribution at a given temperature ratio, the cold distribution is used to calculate the primary combustion zone temperature. Strictly, a method of successive approximation should be used to allow for small redistributions of airflow but the magnitude of the errors involved and the general accuracy of the method as a whole do not warrant it.

Calculation of Individual Loss Factors

(1) Expansion ratio through primary orifice

$$= \frac{2 \cdot 91}{0 \cdot 84} = 3 \cdot 47, \text{ i.e., } m = 0 \cdot 312 .$$

From Fig. 11

$$C_d = 0 \cdot 6 \times 1 \cdot 058 = 0 \cdot 635 .$$

The effect of the shoulder will certainly reduce the discharge and a C_d of $0 \cdot 6$ is used.

Loss through orifice $$= (\lambda - 1)^2 = \left(\frac{3 \cdot 47}{0 \cdot 6} - 1\right)^2 = 22 \cdot 8 .$$

In terms of reference area $$\phi = 22 \cdot 8 \times \left(\frac{38 \cdot 5}{2 \cdot 91}\right)^2 = 3{,}990 .$$

Considering the swirler

$$\alpha = 54 \text{ deg} \quad A_F = 21 \cdot 3 \text{ in.}^2 \quad A_s = 2 \cdot 6 \text{ in.}^2$$

By equation (12)

$$\Phi_F = 1 \cdot 15 \left(\frac{21 \cdot 3}{2 \cdot 6}\right)^2 \frac{1}{(0 \cdot 5878)^2} - 1$$

In terms of reference area $$\phi = 222 \times \left(\frac{38 \cdot 5}{21 \cdot 3}\right)^2$$

$$= 725 .$$

The overall loss for the two resistances in series is the algebraic sum of the loss factors (when expressed in terms of the same area).

Loss through No. 1 *Circuit* $= \phi_1 = 4{,}715$.

(2) Loss through corrugated spacer:

$$\text{Free area} = 1 \cdot 07 \text{ in.}^2$$

$$\text{Expanded area} = 2 \cdot 43 \text{ in.}^2$$

from section 7.3 $$C_d = 0 \cdot 8 .$$

$$\text{Loss in terms of reference area} = \left(\frac{2 \cdot 43}{1 \cdot 07 \times 0 \cdot 8} - 1\right)^2 \left(\frac{38 \cdot 5}{2 \cdot 43}\right)^2 = 850 .$$

' Expansion ' loss after spacer in terms of reference are

$$= \left\{\left(\frac{21 \cdot 3}{2 \cdot 43}\right) - 1\right\}^2 \left(\frac{38 \cdot 5}{21 \cdot 3}\right)^2 = 197$$

Loss through No. 2 Circuit $= \phi_2 = 1{,}047.$

(3) Loss through primary holes:

Firstly, the C_d of the holes must be estimated by the method outlined in section 5.1 and Fig. 17.

F is determined on an area basis only

$$F = \frac{100 \times 1 \cdot 39}{1 \cdot 39 + 0 \cdot 48 + 0 \cdot 55 + 3 \cdot 49 + 1 \cdot 99 + 3 \cdot 49}$$

$$= \frac{139}{11 \cdot 39} = 12 \cdot 2 \text{ per cent .}$$

$$B = \frac{1 \cdot 39}{16 \cdot 6} = 0 \cdot 0837$$

$$\frac{F}{B} = \frac{12 \cdot 2}{0 \cdot 0837} = 146 \, .$$

From Fig. 17 $\qquad C_d = 0 \cdot 582 \, .$

$$\text{Loss in terms of reference area} = \left(\frac{21 \cdot 3}{1 \cdot 39 \times 0 \cdot 582} - 1\right)^2 \left(\frac{38 \cdot 5}{21 \cdot 3}\right)^2$$

$$\underline{\phi_3 = 2{,}090 \, .}$$

(4) Loss through first row of cooling holes:

$$F = \frac{100 \times 0 \cdot 48}{10 \cdot 0} = 4 \cdot 80 \text{ per cent}$$

$$B = \frac{0 \cdot 48}{16 \cdot 6} = 0 \cdot 0289$$

$$\frac{F}{B} = \frac{4 \cdot 80}{0 \cdot 0289} = 166 \, .$$

From Fig. 17 $\qquad C_d = 0 \cdot 595 \, .$

Since these holes are inclined at an angle of 17 deg the discharge coefficient is increased (*see* section 5.1 and Fig. 13).

$$C_d = 0 \cdot 595 \times \sqrt{\left(\frac{1 \cdot 482}{1 \cdot 442}\right)} = 0 \cdot 603 \, .$$

It is assumed that the air entering these holes forms an annular sheath which does not substantially increase in thickness as it flows downstream.

$$\text{Loss factor } \phi_4 = \left(\frac{23 \cdot 8 - 21 \cdot 3}{0 \cdot 603 \times 0 \cdot 48} - 1\right)^2 \left(\frac{38 \cdot 5}{2 \cdot 5}\right)^2 = 13{,}800$$

$$\underline{\phi_4 = 13{,}800 \, .}$$

(5) Loss through second set of cooling holes:

$$F = \frac{100 \times 0 \cdot 55}{9 \cdot 52} = 5 \cdot 78 \text{ per cent}$$

$$B = \frac{0 \cdot 55}{14 \cdot 1} = 0 \cdot 039$$

$$\frac{F}{B} = \frac{5 \cdot 78}{0 \cdot 039} = 148 \, .$$

From Fig. 17 $\qquad C_d = 0 \cdot 585 \, .$

Since holes are inclined at 20 deg, from Fig. 13, C_d is increased.

$$C_d = 0\cdot585 \times \sqrt{\frac{1\cdot482}{1\cdot426}} = 0\cdot596$$

assuming the air forms an annular sheath as before

$$\phi_5 = \left(\frac{26\cdot6 - 23\cdot8}{0\cdot596 \times 0\cdot55} - 1\right)^2 \left(\frac{38\cdot5}{2\cdot8}\right)^2 = 10{,}700\,.$$

$$\underline{\phi_5 = 10{,}700\,.}$$

(6) Loss through first row of mixing holes:

$$F = \frac{100 \times 3\cdot49}{8\cdot975} = 38\cdot9 \text{ per cent}$$

$$B = \frac{3\cdot49}{11\cdot3} = 0\cdot309$$

$$\frac{F}{B} = \frac{38\cdot9}{0\cdot309} = 126\,.$$

From Fig. 17 $\quad C_d = 0\cdot564\,.$

$$\text{Mixing loss} = \tfrac{1}{2}\rho\left(\frac{V_h}{C_d}\right)^2.$$

Therefore

$$\phi_6 = \left(\frac{1}{0\cdot564}\right)^2 \left(\frac{38\cdot5}{3\cdot49}\right)^2 = 383$$

$$\underline{\phi_6 = 383\,.}$$

(7) Loss through third set of cooling holes:

$$F = \frac{100 \times 1\cdot99}{1\cdot99 + 3\cdot49} = \frac{199}{5\cdot48} = 36\cdot3 \text{ per cent}$$

$$B = \frac{1\cdot99}{11\cdot3} = 0\cdot176$$

$$\frac{F}{B} = \frac{36\cdot3}{0\cdot176} = 206$$

$$C_d = 0\cdot608\,.$$

Since inclination is 20 deg C_d is further increased. From Fig. 13

$$C_d = 0\cdot608 \times \sqrt{\left(\frac{1\cdot482}{1\cdot426}\right)} = 0\cdot62\,.$$

By equation (41) the loss factor in terms of the hole

$$\text{area} = \left(\frac{1}{0\cdot62}\right)^2 = 2\cdot6$$

$$\phi_7 = 2\cdot6\left(\frac{38\cdot5}{1\cdot99}\right)^2 = 974$$

$$\underline{\phi_7 = 974\,.}$$

Equation (41) was used as it is very difficult to decide to which effective area the injected air eventually ' expands '.

(8) Loss through final mixing holes:

$$F = 100 \text{ per cent}$$

$$B = \frac{3\cdot 49}{8\cdot 3} = 0\cdot 42$$

$$\frac{F}{B} = \frac{100}{0\cdot 42} = 238\,.$$

Therefore $C_d = 0\cdot 61\,.$

$$\phi_8 = \left(\frac{1}{0\cdot 61}\right)^2\left(\frac{38\cdot 5}{3\cdot 49}\right)^2 = 327$$

$$\underline{\phi_8 = 327}\,.$$

Cold air distribution :

$$\begin{array}{ll} \phi_1 = 4{,}715 & \sqrt{\phi_1} = 68\cdot 7 \\ \phi_2 = 1{,}047 & \sqrt{\phi_2} = 32\cdot 4 \\ \phi_3 = 2{,}090 & \sqrt{\phi_3} = 45\cdot 7 \\ \phi_4 = 13{,}800 & \sqrt{\phi_4} = 117\cdot 6 \\ \phi_5 = 10{,}700 & \sqrt{\phi_5} = 107\cdot 0 \\ \phi_6 = 383 & \sqrt{\phi_6} = 19\cdot 6 \\ \phi_7 = 974 & \sqrt{\phi_7} = 31\cdot 2 \\ \phi_8 = 327 & \sqrt{\phi_8} = 18\cdot 1\,. \end{array}$$

By equation (51)

$$W_1 = \frac{100}{1 + \frac{68\cdot 7}{32\cdot 4} + \frac{68\cdot 7}{45\cdot 7} + \frac{68\cdot 7}{117\cdot 6} + \frac{68\cdot 7}{107\cdot 0} + \frac{68\cdot 7}{19\cdot 6} + \frac{68\cdot 7}{31\cdot 2} + \frac{68\cdot 7}{18\cdot 1}}$$

$$= \frac{100}{1 + 2\cdot 12 + 1\cdot 50 + 0\cdot 58 + 0\cdot 64 + 3\cdot 51 + 2\cdot 20 + 3\cdot 80} = \frac{100}{15\cdot 35}$$

$\underline{W_1 = 6\cdot 5 \text{ per cent.}}$

$$W_2 = \frac{100}{\frac{32\cdot 4}{68\cdot 7} + 1 + \frac{32\cdot 4}{45\cdot 7} + \frac{32\cdot 4}{117\cdot 6} + \frac{32\cdot 4}{107\cdot 0} + \frac{32\cdot 4}{19\cdot 6} + \frac{32\cdot 4}{31\cdot 2} + \frac{32\cdot 4}{18\cdot 1}}$$

$$= \frac{100}{0\cdot 47 + 1 + 0\cdot 71 + 0\cdot 27 + 0\cdot 30 + 1\cdot 65 + 1\cdot 04 + 1\cdot 79} = \frac{100}{7\cdot 23}$$

$\underline{W_2 = 13\cdot 8 \text{ per cent.}}$

$$W_3 = \frac{100}{\frac{45\cdot 7}{68\cdot 7} + \frac{45\cdot 7}{32\cdot 4} + 1 + \frac{45\cdot 7}{117\cdot 6} + \frac{45\cdot 7}{107\cdot 0} + \frac{45\cdot 7}{19\cdot 6} + \frac{45\cdot 7}{31\cdot 2} + \frac{45\cdot 7}{18\cdot 1}}$$

$$= \frac{100}{0\cdot 66 + 1\cdot 42 + 1 + 0\cdot 39 + 0\cdot 43 + 2\cdot 34 + 1\cdot 47 + 2\cdot 53} = \frac{100}{10\cdot 24}$$

$\underline{W_3 = 9\cdot 8 \text{ per cent.}}$

$$W_4 = \frac{100}{\frac{117\cdot6}{68\cdot7} + \frac{117\cdot6}{32\cdot4} + \frac{117\cdot6}{45\cdot7} + 1 + \frac{117\cdot6}{107} + \frac{117\cdot6}{19\cdot6} + \frac{117\cdot6}{31\cdot2} + \frac{117\cdot6}{18\cdot1}}$$

$$= \frac{100}{1\cdot71 + 3\cdot63 + 2\cdot57 + 1 + 1\cdot10 + 6\cdot00 + 3\cdot77 + 6\cdot50} = \frac{100}{26\cdot28}$$

$W_4 = 3\cdot8$ per cent.

$$W_5 = \frac{100}{\frac{107}{68\cdot7} + \frac{107}{32\cdot4} + \frac{107}{45\cdot7} + \frac{107}{117\cdot6} + 1 + \frac{107}{19\cdot6} + \frac{107}{31\cdot2} + \frac{107}{18\cdot1}}$$

$$= \frac{100}{1\cdot56 + 3\cdot30 + 2\cdot34 + 0\cdot91 + 1 + 5\cdot42 + 3\cdot43 + 5\cdot90} = \frac{100}{23\cdot86}$$

$W_5 = 4\cdot2$ per cent.

$$W_6 = \frac{100}{\frac{19\cdot6}{68\cdot7} + \frac{19\cdot6}{32\cdot4} + \frac{19\cdot6}{45\cdot7} + \frac{19\cdot6}{117\cdot6} + \frac{19\cdot6}{107} + 1 + \frac{19\cdot6}{31\cdot2} + \frac{19\cdot6}{18\cdot1}}$$

$$= \frac{100}{0\cdot28 + 0\cdot60 + 0\cdot43 + 0\cdot17 + 0\cdot18 + 1 + 0\cdot63 + 1\cdot08} = \frac{100}{4\cdot37}$$

$W_6 = 22\cdot8$ per cent.

$$W_7 = \frac{100}{\frac{31\cdot2}{68\cdot7} + \frac{31\cdot2}{32\cdot4} + \frac{31\cdot2}{45\cdot7} + \frac{31\cdot2}{117\cdot6} + \frac{31\cdot2}{107\cdot0} + \frac{31\cdot2}{19\cdot6} + 1 + \frac{31\cdot2}{18\cdot1}}$$

$$= \frac{100}{0\cdot45 + 0\cdot96 + 0\cdot68 + 0\cdot26 + 0\cdot29 + 1\cdot59 + 1 + 1\cdot72} = \frac{100}{6\cdot95}$$

$W_7 = 14\cdot4$ per cent.

$$W_8 = \frac{100}{\frac{18\cdot1}{68\cdot7} + \frac{18\cdot1}{32\cdot4} + \frac{18\cdot1}{45\cdot7} + \frac{18\cdot1}{117\cdot6} + \frac{18\cdot1}{107\cdot0} + \frac{18\cdot1}{19\cdot6} + \frac{18\cdot1}{31\cdot2} + 1}$$

$$= \frac{100}{0\cdot26 + 0\cdot56 + 0\cdot40 + 0\cdot15 + 0\cdot17 + 0\cdot92 + 0\cdot58 + 1} = \frac{100}{4\cdot04}$$

$W_8 = 24\cdot7$ per cent.

Check: $6\cdot5 + 13\cdot8 + 9\cdot8 + 3\cdot8 + 4\cdot2 + 22\cdot8 + 14\cdot4 + 24\cdot7 = 100$ per cent.

Overall cold loss factor by Equation (50)

$$\Phi = \phi_1\left(\frac{W_1}{W}\right)^2 = 4{,}715\left(\frac{6\cdot5}{100}\right)^2 = 19\cdot9$$

$= 19\cdot9$ in terms of reference velocity heads.

Check: $$\Phi = \phi_2\left(\frac{W_2}{W}\right)^2 = 1{,}047\left(\frac{13\cdot8}{100}\right)^2 = 19\cdot9\,.$$

The measured value of the cold pressure loss factor was $20\cdot7$ an error of about 4 per cent.

Hot pressure loss

To determine the effect of heat addition it is necessary to arrive at a value for the primary temperature.

Using the previously determined air flow distribution and assuming circuits 1, 2 and 3 constitute the primary air flow.

Percentage primary air $= 6\cdot5 + 13\cdot8 + 9\cdot8 = 30\cdot1$ per cent.

Neglecting specific heat variation and assuming :—

Inlet temperature $= 200$ deg C.

Outlet temperature $= 700$ deg C.

If T_1 is the primary absolute temperature

then $30\cdot1T_1 + 69\cdot9 \times 473 = 100 \times 973$

therefore $$T_1 = \frac{97{,}300 - 33{,}000}{30\cdot1} = \frac{64{,}300}{30\cdot1}$$

$$= 2{,}130 \text{ deg } K.$$

By equation (42a)

$$\text{Heat addition loss factor} = \left(\frac{2{,}130}{473} - 1\right)$$

and in terms of reference area

$$= \left(\frac{1{,}657}{473}\right)\left(\frac{38\cdot5}{21\cdot3}\right)^2 = 11\cdot4\,.$$

Overall primary loss factor excluding combustion loss is by equation (50)

$$\phi_p = \Phi\left(\frac{W}{W_1 + W_2 + W_3}\right)^2 = 19\cdot9\left(\frac{100}{30\cdot1}\right)^2 = \frac{19\cdot9}{0\cdot301^2} = 220\,.$$

New primary loss factor including combustion loss will be $220 + 11\cdot4 = 231\cdot4$.

Assuming the secondary loss factor remains constant

$$\phi_s = \frac{19\cdot9}{(0\cdot699)^2} = 40\cdot8\,.$$

Therefore the new distribution is

$$Q_p\sqrt{(231\cdot4)} = Q_s\sqrt{(40\cdot8)}\,.$$

Thus percentage through primary

$$= \frac{100}{1 + \sqrt{\left(\frac{231\cdot4}{40\cdot8}\right)}} = 29\cdot5 \text{ per cent}\,.$$

Thus heat addition has reduced the primary total flow by $30\cdot1 - 29\cdot5 = 0\cdot6$ per cent.

The new hot loss factor $= 231\cdot4(0\cdot295)^2 = 20\cdot2$

The measured hot loss factor for the assumed temperature rise was 25, an error of about 20 per cent.

APPENDIX III

Derivation of Theoretical Whirl and Axial Velocity Distributions

The equation for radial equilibrium in vortex flow is

$$\frac{1}{\rho}\frac{dp}{dr} = \frac{V_w^2}{r} \quad \ldots \quad (1)$$

The total energy/unit mass at any radius r is given by Bernoulli's equation for a compressible fluid

$$H = \frac{V_a^2}{2} + \frac{V_w^2}{2} + \frac{\gamma}{\gamma - 1}\frac{p}{\rho}. \quad \ldots \quad (2)$$

Assuming the expansion to be

$$\frac{p}{\rho\gamma} = \text{constant} \quad \ldots \quad (3)$$

and that H is constant, we have by differentiating (2) and (3) that

$$V_a\frac{dV_a}{dr} + V_w\frac{dV_w}{dr} + \frac{1}{\rho}\frac{dp}{dr} = 0$$

and using (1)

$$V_a\frac{dV_a}{dr} + V_w\frac{dV_w}{dr} + \frac{V_w^2}{r} = 0. \quad \ldots \quad (4)$$

The general vortex law is

$$V_w r^n = C \quad \ldots \quad (5)$$

and also

$$\tan\alpha = \frac{V_w}{V_a} \quad \ldots \quad (6)$$

and (5) and (6)

$$V_a \tan\alpha \,.\, r^n = C. \quad \ldots \quad (7)$$

By differentiation

$$\tan\alpha \,.\, r^n\frac{dV_a}{dr} + V_a\tan\alpha \,.\, nr^{n-1} + V_a r^n\sec^2\alpha\frac{d\alpha}{dr} = 0$$

whence

$$\frac{d\alpha}{dr} = -\tfrac{1}{2}\sin 2\alpha\left(\frac{1}{V_a}\frac{dV_a}{dr} + \frac{n}{r}\right). \quad \ldots \quad (8)$$

Differentiating (6)

$$\frac{dV_w}{dr} = \frac{dV_a}{dr}\tan\alpha + V_a\sec^2\alpha\frac{d\alpha}{dr}.$$

Therefore

$$V_w\frac{dV_w}{dr} = V_a\frac{dV_a}{dr}\tan^2\alpha + V_a^2\sec^2\alpha\tan\alpha\frac{d\alpha}{dr}. \quad \ldots \quad (9)$$

Substituting for $d\alpha/dr$ in (9) and then substituting for $V_w \,.\, dV_w/dr$ and V_w^2/r in (4) finally gives

$$V_a\frac{dV_a}{dr} + (1-n)C^2 r^{-(2n+1)} = 0.$$

Integrating, using subscript $_0$ to refer to conditions at the inner radius for convenience

$$V_a^2 = V_{a0}^2 + C^2\frac{(1-n)}{n}\left[\frac{1}{r^{2n}} - \frac{1}{r_0^{2n}}\right]. \quad \ldots \quad (10)$$

Free vortex blading

For free vortex flow $n = 1$.

Therefore from equation (10) $V_a = V_{a0} = \text{constant}$

and by equation (7)

$$\tan \alpha = \frac{J}{r} \text{ where } J = \text{constant} = \frac{C}{V_{a0}}.$$

Now
$$\sec^2 \alpha_m = 1 + \frac{C^2}{r_m^2 V_a^2}$$

and the weighted mean radius $= r_m = \dfrac{1}{\sqrt{2}} (R^2 + r_0^2)^{1/2}$.

Therefore
$$\sec^2 \alpha_m = 1 + \frac{2r_0^2 \tan^2 \alpha_0}{R^2 + r_0^2}. \qquad (11)$$

Forced vortex blading

For forced vortex flow $n = -1$.

Therefore from equation (10) $V_a^2 = V_{a0}^2 - 2C^2(r^2 - r_0^2)$

and
$$\tan \alpha = \frac{C_r}{\sqrt{\{V_{a0}^2 - 2C^2(r^2 - r_0^2)\}}}.$$

Therefore
$$\tan \alpha_m = \frac{r_m}{\sqrt{\left\{\dfrac{r_0^2}{\tan^2 \alpha_0} - 2(r_m^2 - r_0^2)\right\}}}$$

$$\sec^2 \alpha_m = 1 + \left[\frac{(R^2 + r_0^2)}{2\left\{\dfrac{r_0^2}{\tan^2 \alpha_0} - (R^2 - r_0^2)\right\}}\right]$$

$$= 1 + \frac{(R^2 + r_0^2) \tan^2 \alpha_0}{2\{r_0^2 \sec^2 \alpha_0 - R^2 \tan^2 \alpha_0\}}$$

$$= 1 + \left\{\frac{(R^2 + r_0^2}{2(r_0^2 \operatorname{cosec}^2 \alpha_0 - R^2)}\right\}. \qquad (12)$$

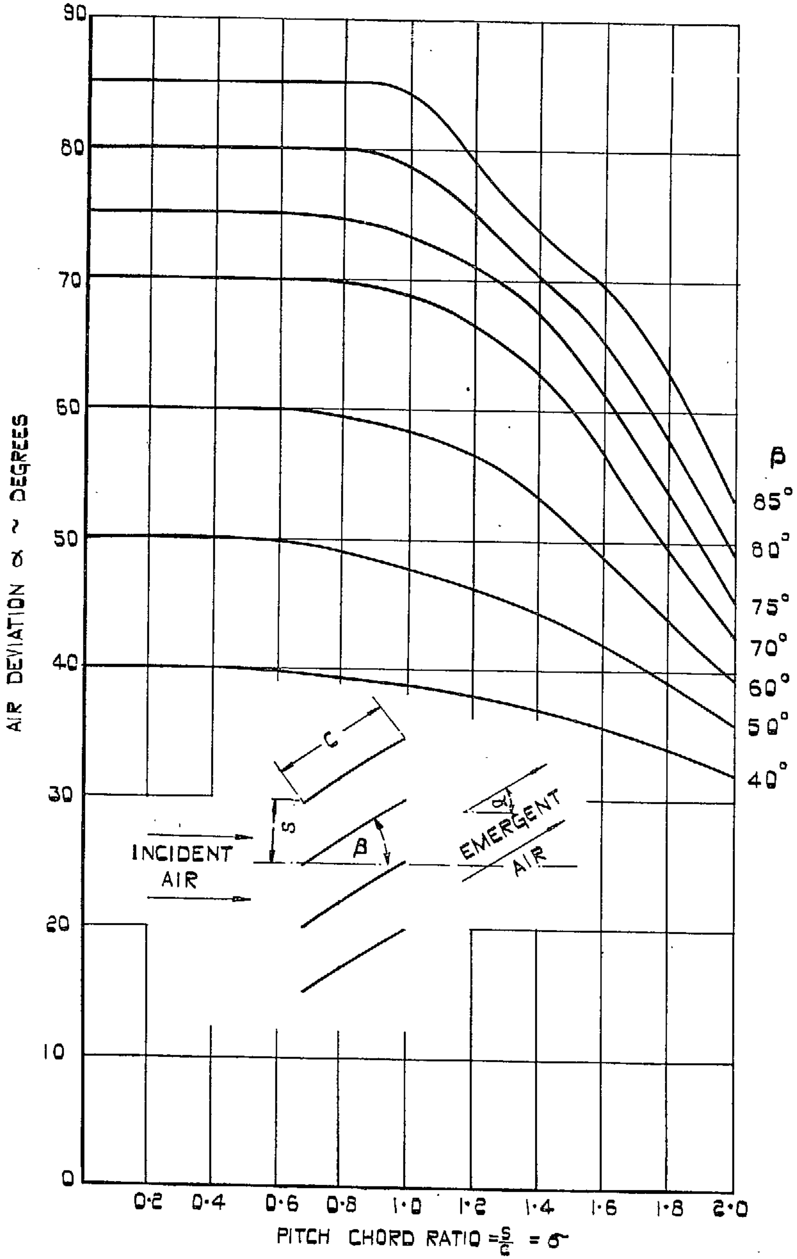

FIG. 1. Variation of air outlet angle for flat plate cascades.

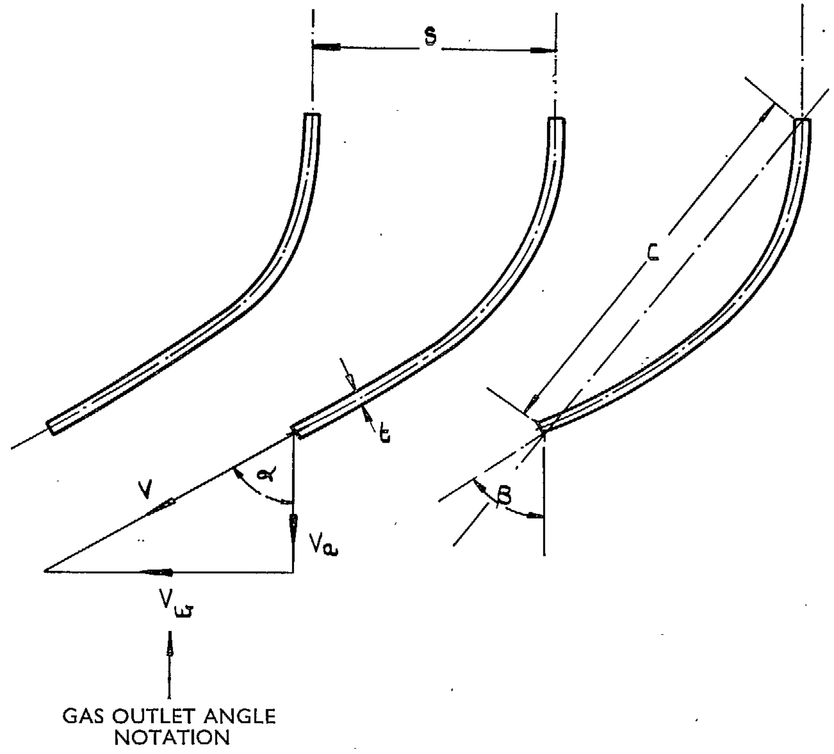

FIG. 2. Swirler blade nomenclature.

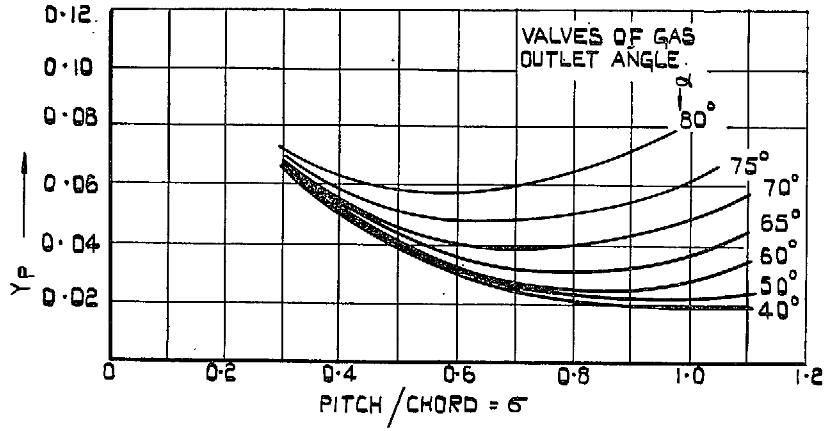

FIG. 3. Profile loss coefficients for zero incidence. (t/c = 20 per cent. $R_e = 2 \times 10^5$. $M < 0{\cdot}6$.)

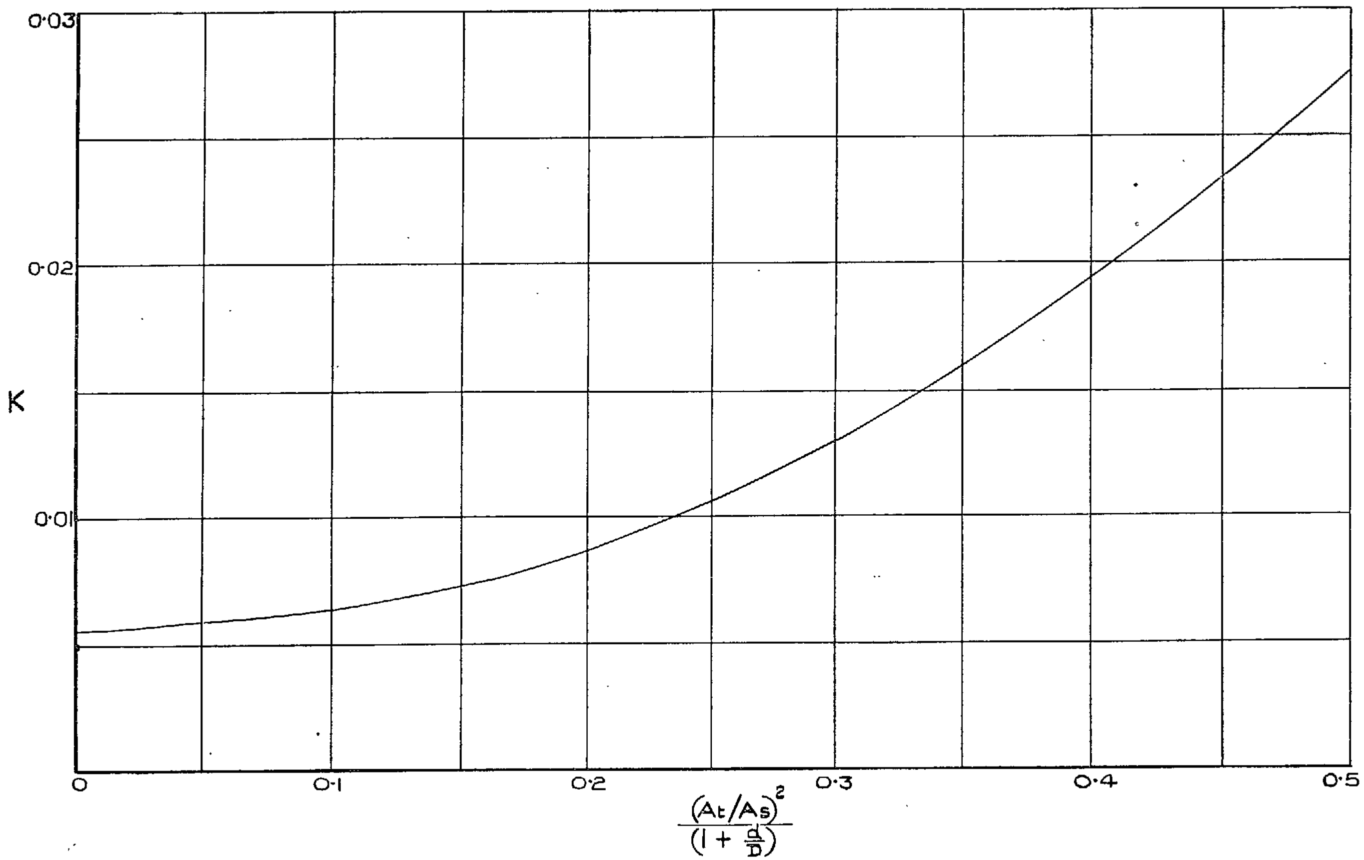

FIG. 4. Secondary losses in blades.

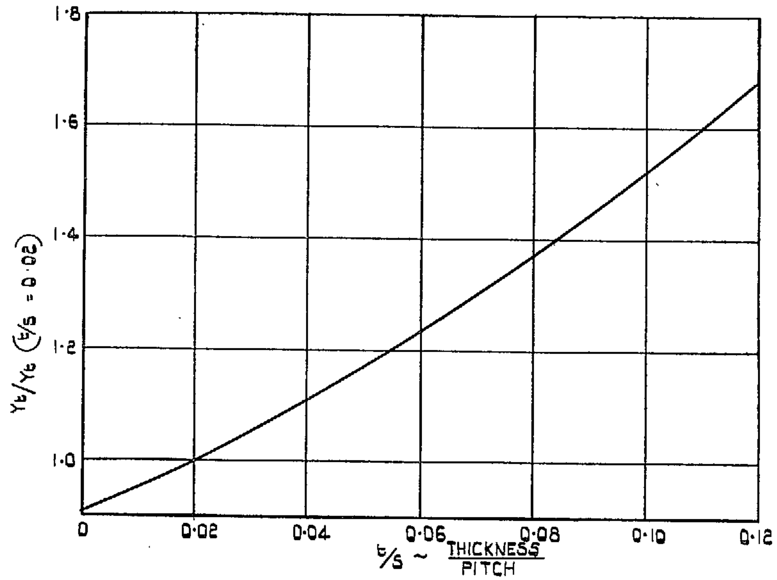

FIG. 5. Effect of trailing-edge thickness on blade loss coefficient.

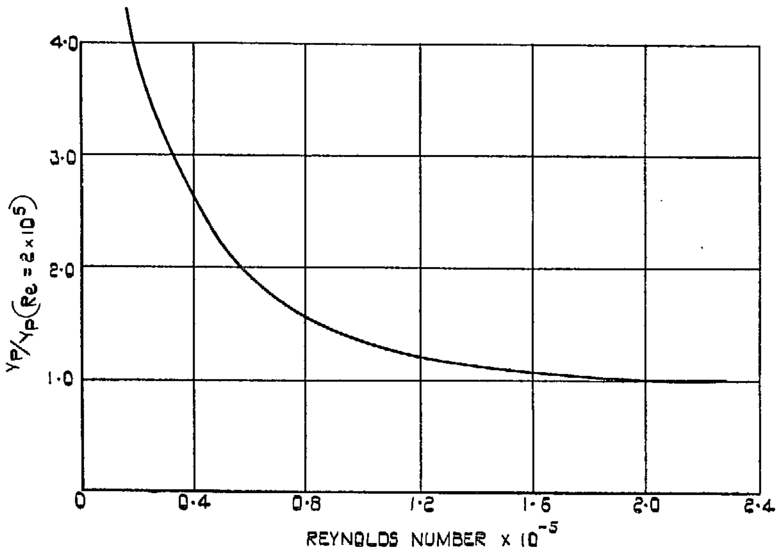

FIG. 6. Variation of profile loss with Reynolds number.

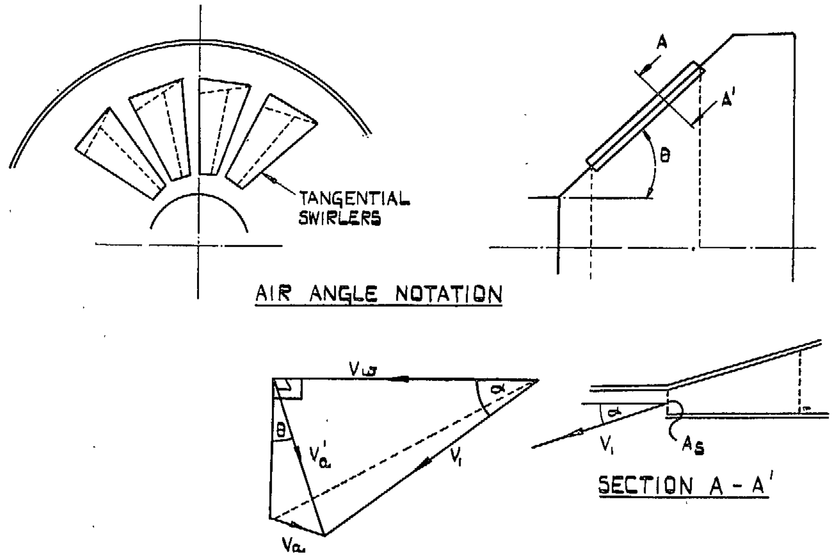

FIG. 7. Ported swirler.

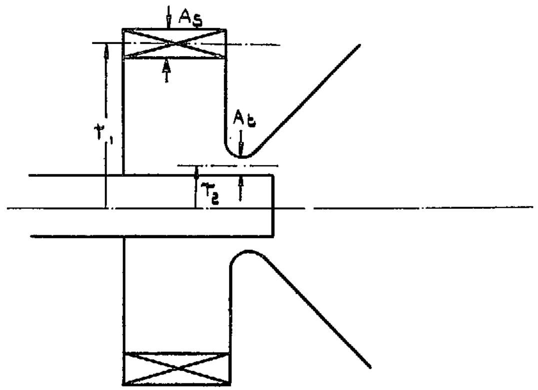

FIG. 8. Vortex-type swirler.

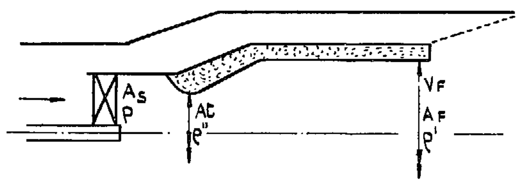

FIG. 9. Notational diagram (*see* section 2·3).

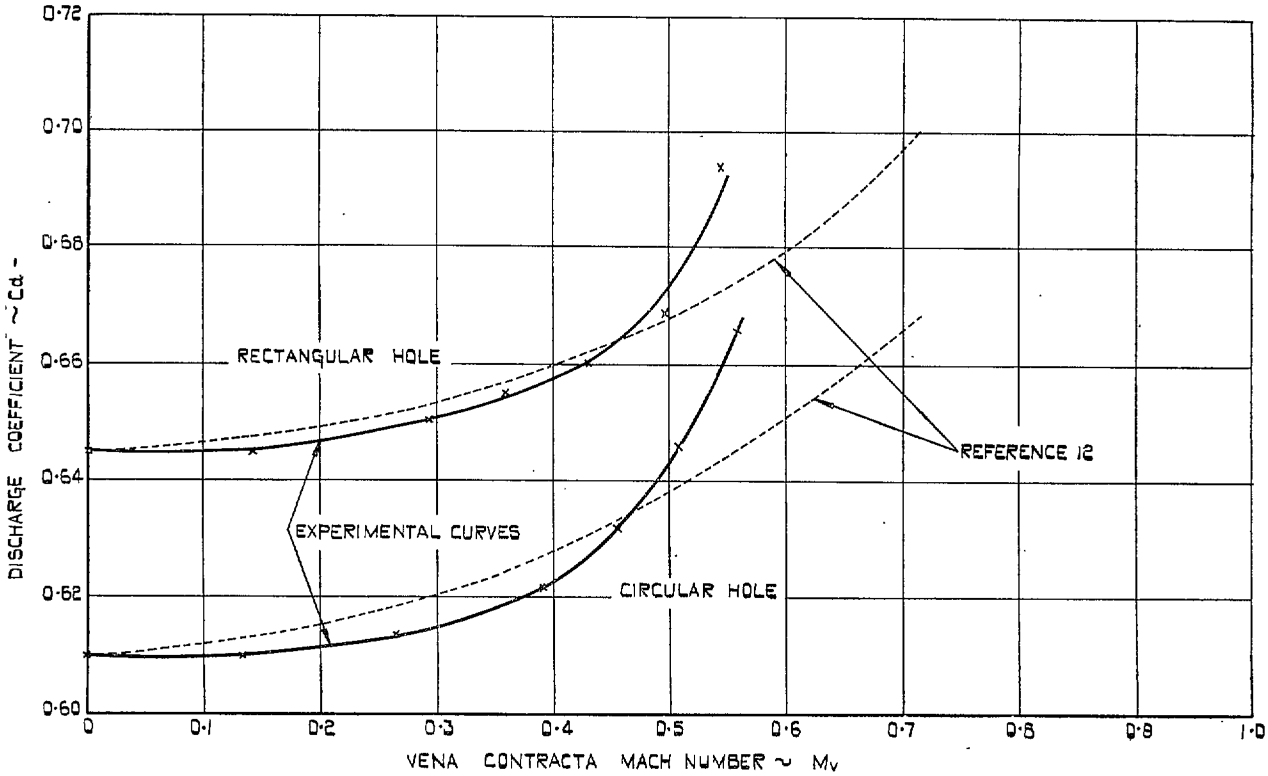

FIG. 10. Variation of discharge coefficient with vena-contracta Mach number.

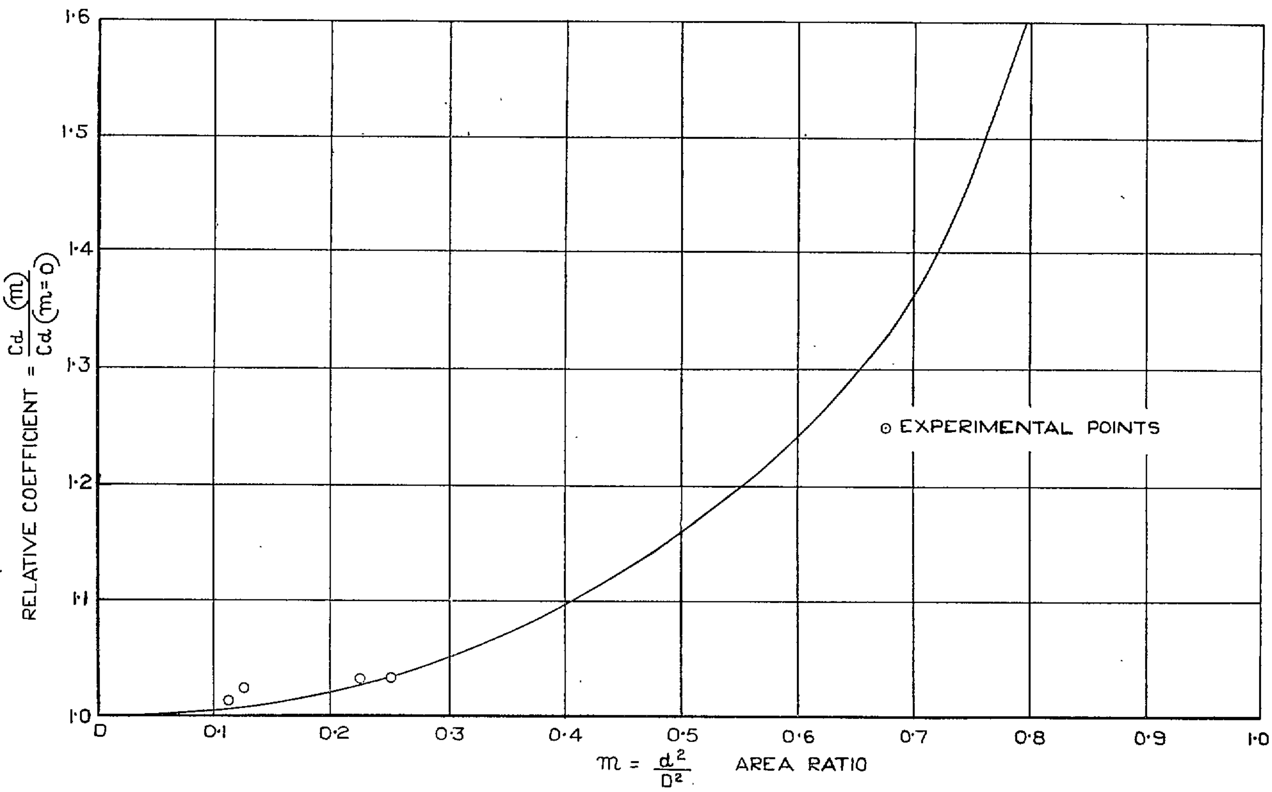

FIG. 11. Relative discharge coefficient *vs.* area ratio.

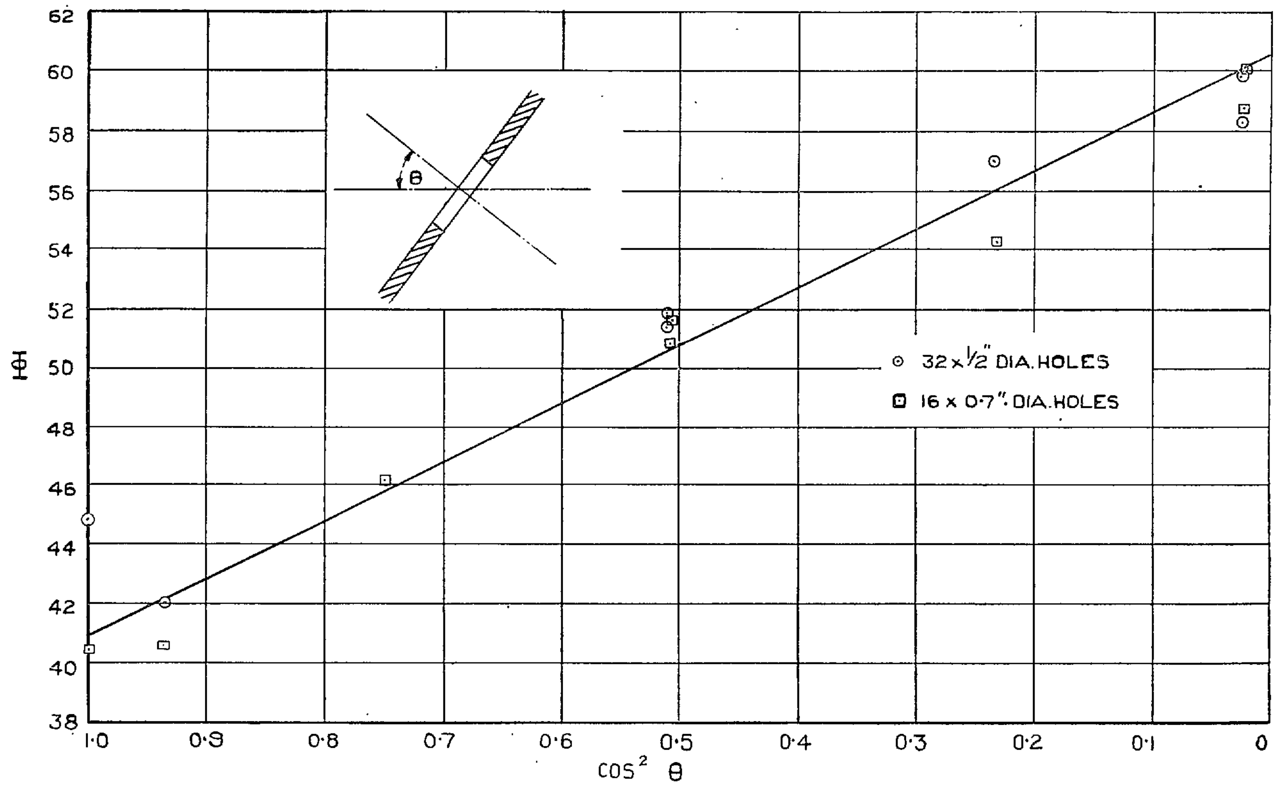

FIG 12. Variation of loss coefficient with hole inclination.

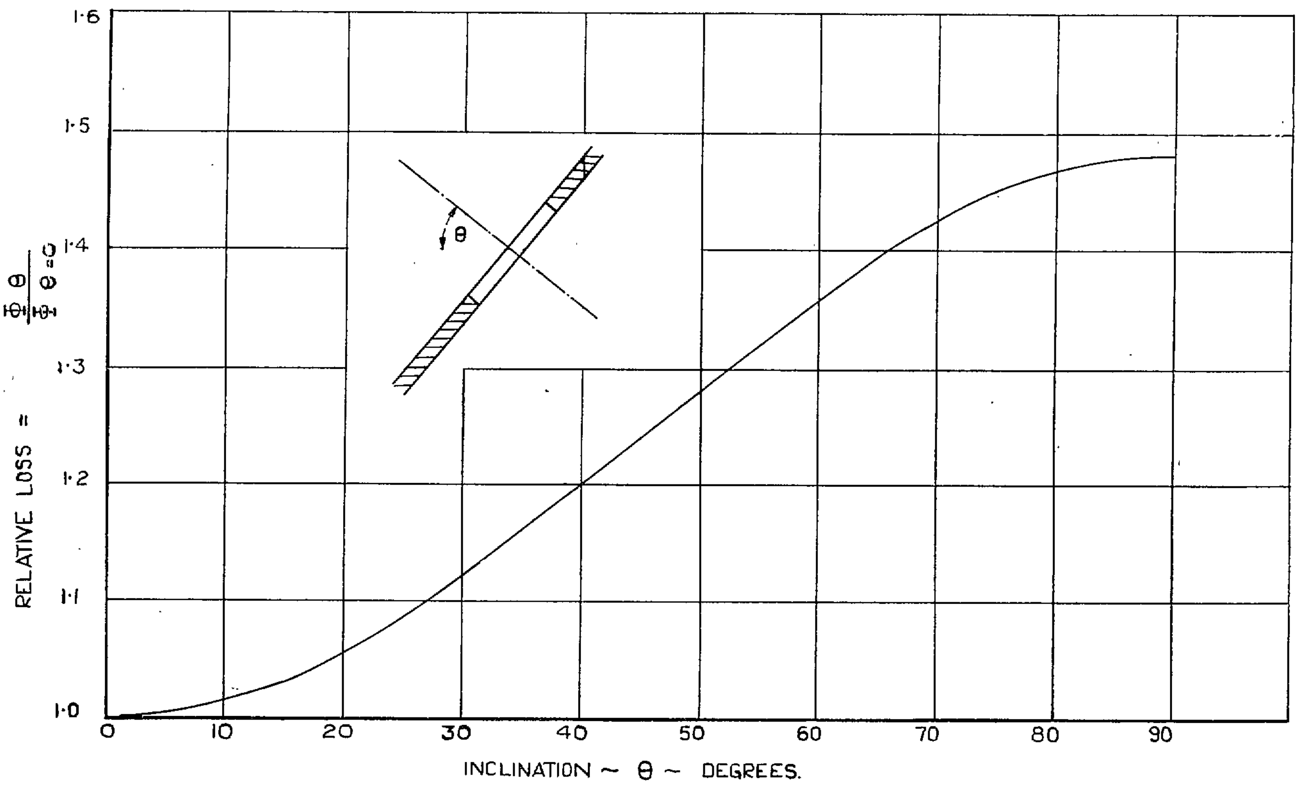

FIG. 13. Relative loss *vs.* hole inclination.

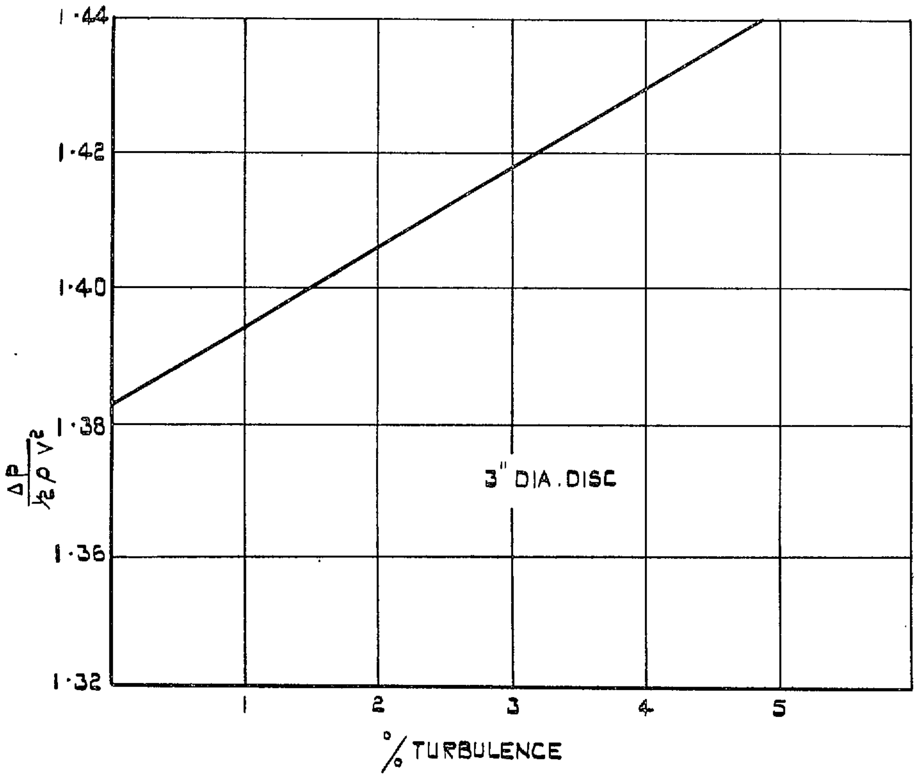

Fig. 14. Variation of static pressure drop coefficient with percentage turbulence. (From Ref. 14.)

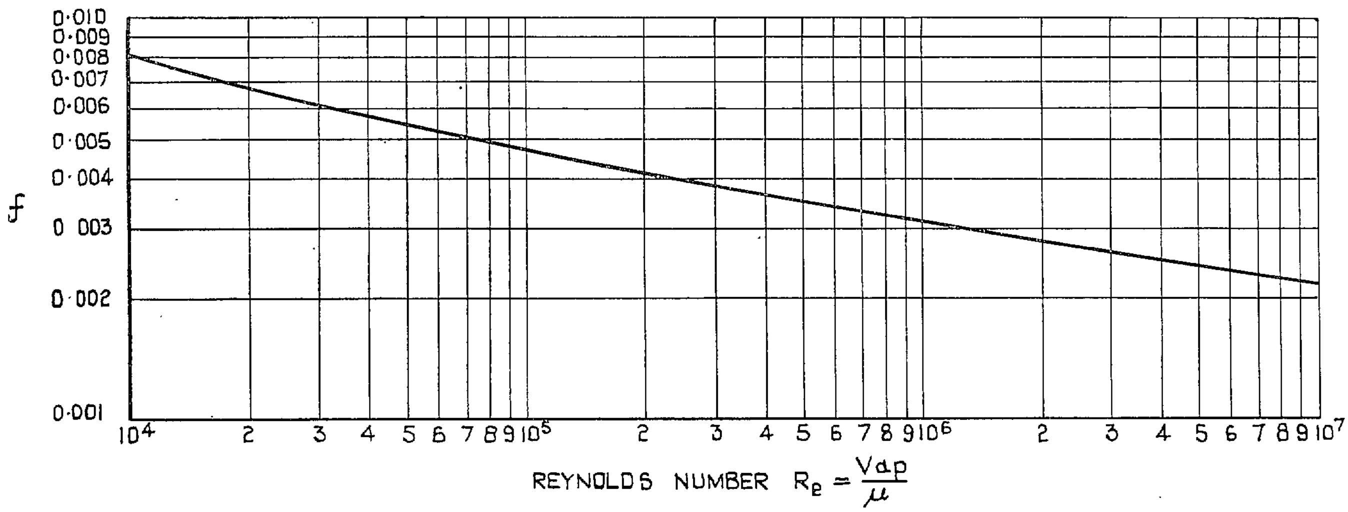

Fig. 15. Friction factor f for sheet metal surfaces *vs.* Reynolds number.

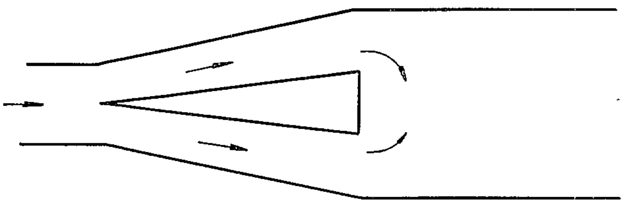

FIG. 16a. Conventional or 'plain' gutter.

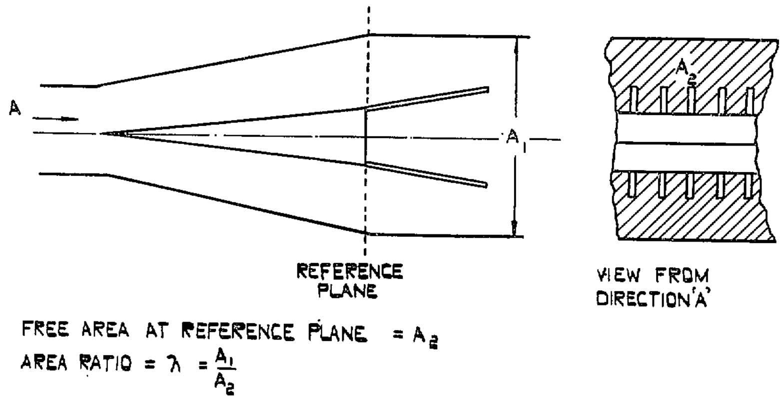

FIG. 16c. Notation for 'finger' flame spreaders.

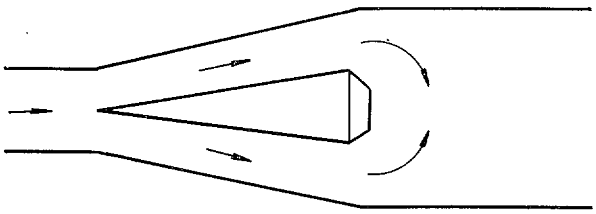

FIG. 16b. 'Skirted' gutter.

FIG. 16. Gutter notation.

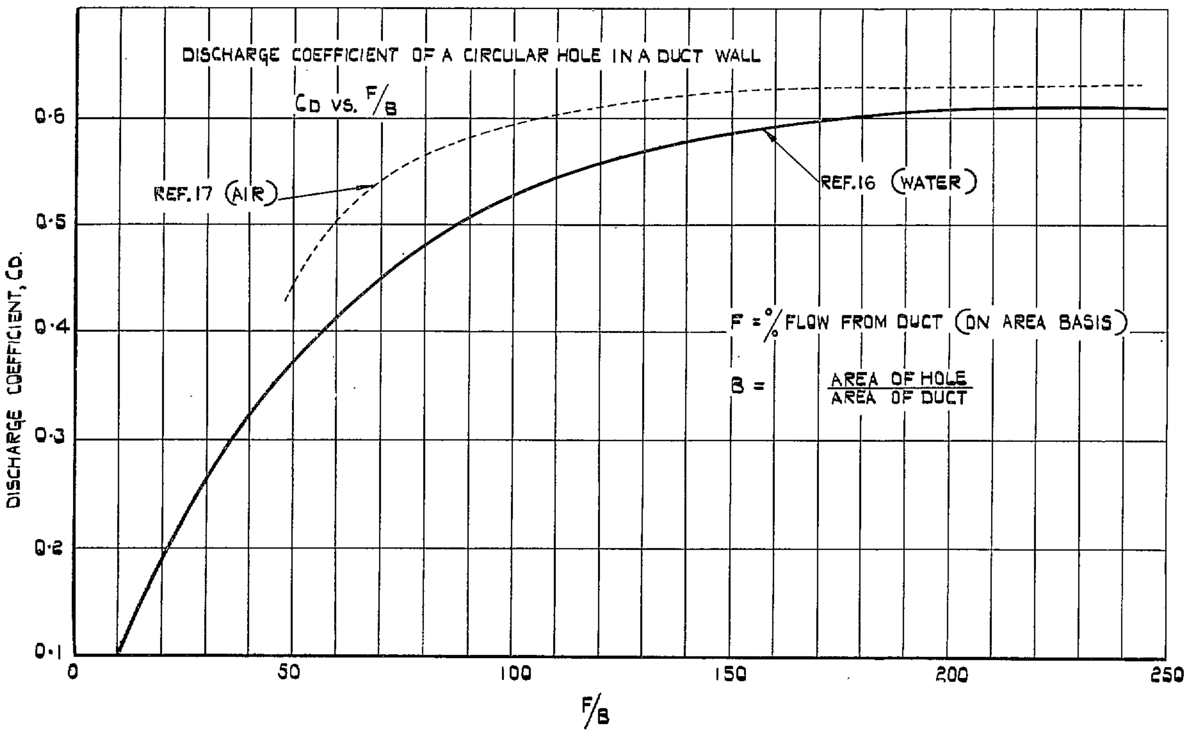

FIG. 17. C_d for hole in wall of duct.

(4522) Wt. 20/9036 K.7 5/57 Hw.

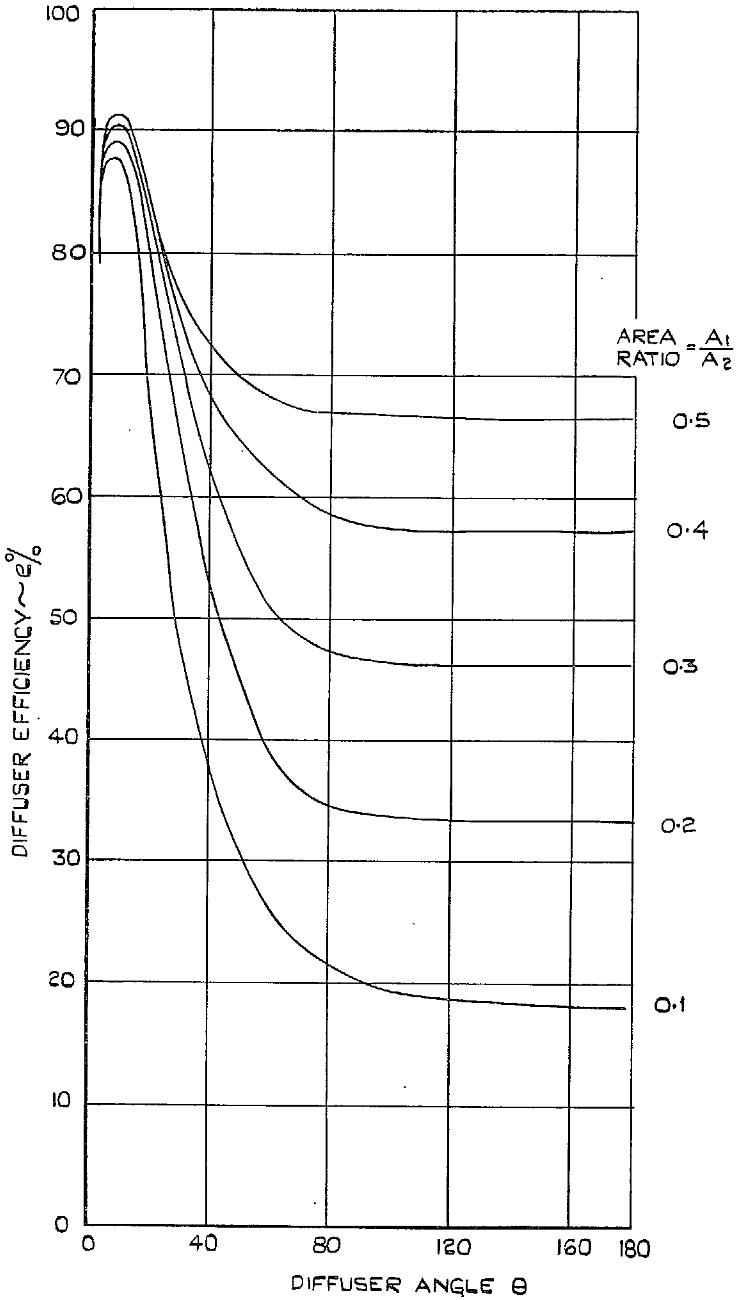

FIG. 18. Diffuser efficiency e *vs.* diffuser angle θ.

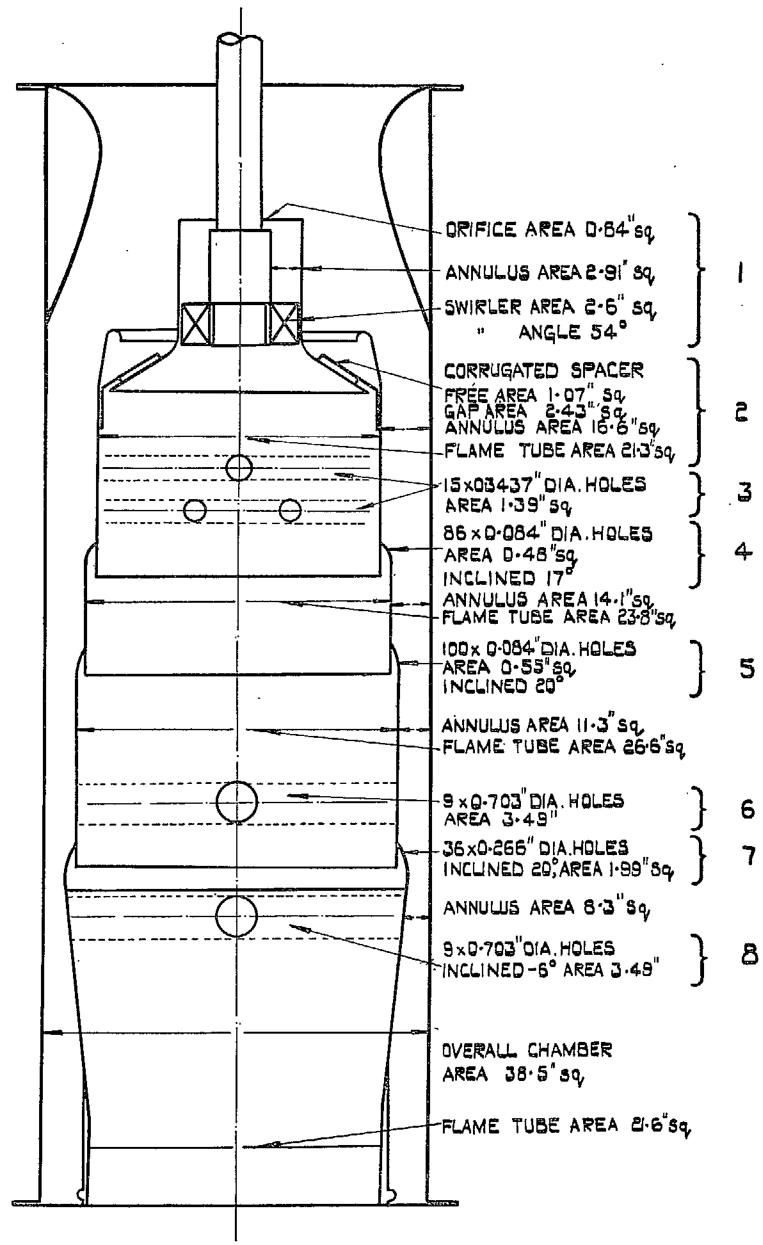

FIG. 19. Diagram of conventional combustion chamber.

PRINTED IN GREAT BRITAIN

Publications of the Aeronautical Research Council

ANNUAL TECHNICAL REPORTS OF THE AERONAUTICAL RESEARCH COUNCIL (BOUND VOLUMES)

1939 Vol. I. Aerodynamics General, Performance, Airscrews, Engines. 50s. (51s. 9d.).
Vol. II. Stability and Control, Flutter and Vibration, Instruments, Structures, Seaplanes, etc. 63s. (64s. 9d.)

1940 Aero and Hydrodynamics, Aerofoils, Airscrews, Engines, Flutter, Icing, Stability and Control Structures, and a miscellaneous section. 50s. (51s. 9d.)

1941 Aero and Hydrodynamics, Aerofoils, Airscrews, Engines, Flutter, Stability and Control Structures. 63s. (64s. 9d.)

1942 Vol. I. Aero and Hydrodynamics, Aerofoils, Airscrews, Engines. 75s. (76s. 9d.)
Vol. II. Noise, Parachutes, Stability and Control, Structures, Vibration, Wind Tunnels. 47s. 6d. (49s. 3d.)

1943 Vol. I. Aerodynamics, Aerofoils, Airscrews. 80s. (81s. 9d.)
Vol. II. Engines, Flutter, Materials, Parachutes, Performance, Stability and Control, Structures. 90s. (92s. 6d.)

1944 Vol. I. Aero and Hydrodynamics, Aerofoils, Aircraft, Airscrews, Controls. 84s. (86s. 3d.)
Vol. II. Flutter and Vibration, Materials, Miscellaneous, Navigation, Parachutes, Performance, Plates and Panels, Stability, Structures, Test Equipment, Wind Tunnels. 84s. (86s. 3d.)

1945 Vol. I. Aero and Hydrodynamics, Aerofoils. 130s. (132s. 6d.)
Vol. II. Aircraft, Airscrews, Controls. 130s. (132s. 6d.)
Vol. III. Flutter and Vibration, Instruments, Miscellaneous, Parachutes, Plates and Panels, Propulsion. 130s. (132s. 3d.)
Vol. IV. Stability, Structures, Wind Tunnels, Wind Tunnel Technique. 130s. (132s. 3d.)

Annual Reports of the Aeronautical Research Council—

1937 2s. (2s. 2d.) 1938 1s. 6d. (1s. 8d.) 1939–48 3s. (3s. 3d.)

Index to all Reports and Memoranda published in the Annual Technical Reports, and separately—

April, 1950 - - - - - R. & M. 2600 2s. 6d. (2s. 8d.)

Author Index to all Reports and Memoranda of the Aeronautical Research Council—

1909—January, 1954 R. & M. No. 2570 15s. (15s. 6d.)

Indexes to the Technical Reports of the Aeronautical Research Council—

December 1, 1936—June 30, 1939	R. & M. No. 1850	1s. 3d. (1s. 5d.)
July 1, 1939—June 30, 1945	R. & M. No. 1950	1s. (1s. 2d.)
July 1, 1945—June 30, 1946	R. & M. No. 2050	1s. (1s. 2d.)
July 1, 1946—December 31, 1946	R. & M. No. 2150	1s. 3d. (1s. 5d.)
January 1, 1947—June 30, 1947	R. & M. No. 2250	1s. 3d. (1s. 5d.)

Published Reports and Memoranda of the Aeronautical Research Council—

Between Nos. 2251–2349	R. & M. No. 2350	1s. 9d. (1s. 11d.)
Between Nos. 2351–2449	R. & M. No. 2450	2s. (2s. 2d.)
Between Nos. 2451–2549	R. & M. No. 2550	2s. 6d. (2s. 8d.)
Between Nos. 2551–2649	R. & M. No. 2650	2s. 6d. (2s. 8d.)

Prices in brackets include postage

HER MAJESTY'S STATIONERY OFFICE

York House, Kingsway, London W.C.2; 423 Oxford Street, London W.1 (Post Orders: P.O. Box 569, London S.E.1) 13a Castle Street, Edinburgh 2; 39 King Street, Manchester 2; 2 Edmund Street, Birmingham 3; 109 St. Mary Street, Cardiff; Tower Lane, Bristol, 1; 80 Chichester Street, Belfast, *or through any bookseller.*

S.O. Code No. 23-2987

R. & M. No. 2987